

RESEARCH

Open Access



# Metabolome and transcriptome analyses for explore heat stress responses and adaptation mechanisms in *Rhododendron henanense* subsp. *lingbaoense*

Yonghui Li<sup>1</sup>, Xufeng Li<sup>1</sup>, Mengxin Lei<sup>1</sup>, Junwang Han<sup>2</sup>, Ziming Huang<sup>1</sup>, Kai Zhang<sup>2</sup>, Yifan Yang<sup>2</sup>, Ning Yang<sup>1</sup>, Xiangli Yu<sup>1</sup> and Xiaojun Zhou<sup>1\*</sup>

## Abstract

In this study, we aimed to investigate the heat tolerance mechanism in *Rhododendron henanense* subsp. *lingbaoense* (*Rhl*). *Rhl* seedlings were treated at 40°C (RLH), 32°C (RLM), and 24°C (RLC), and the changes in transcriptome and metabolome were compared. Overall, 78 differentially expressed metabolites were detected, and 8450 differentially expressed genes (DEGs) were identified. KEGG analysis revealed that the DEGs in RLH vs. RLC were mainly enriched in photosynthesis, secondary metabolic biosynthesis, and flavonoid biosynthesis. Most genes encoding glutathione-S-transferase were upregulated, whereas genes related to heat shock proteins were significantly downregulated. 31 genes related to photosynthesis were significantly upregulated ( $P$ -value < 0.001). It was speculated that these DEGs are related to the response of *Rhl* to high temperature stress (HTS). Overall, 9 TF families might be the key regulators of Heat stress response pathways in *Rhl*. Mining of DEGs revealed that the expression of some genes related to heat stress function increased highly significantly, e.g., the *Rhe008987* related to Glutathione-S-transferase, *Rhe016769* encoding peroxidase, and *Rhe001827* encoding chalcone and stilbene synthases. Metabolome and transcriptome correlation analysis revealed that three comparison groups (RLH vs. RLC, RLH vs. RLM, and RLM vs. RLC) shared 12 metabolic pathways in which the DEMs were enriched. HTS inhibited or induced expression of genes in flavonoid biosynthesis pathway and led to decrease in kaempferol content and quercetin accumulation. HT induced expression of genes in ABC pathway, which may be one of the reasons for the significant accumulation of L-isoleucine, L-leucine, and L-proline. In this study, DEGs mining found that the expression of some genes related to heat stress function increased highly significantly. And two omics correlation analysis revealed that 12 metabolic pathways were enriched in three comparison groups. These results helped in elucidating the molecular mechanisms of response of *Rhl* to HTS.

**Keywords** *Rhododendron henanense* subsp. *lingbaoense*, High-temperature stress, Transcriptome, Metabolome, Flavonoid biosynthesis, Transcriptome sequencing

\*Correspondence:  
Xiaojun Zhou  
lynubio@126.com

<sup>1</sup>School of Life Sciences, Luoyang Normal University, Luoyang, HN 471934, China

<sup>2</sup>Henan Xiaoqinling National Nature Reserve Management Bureau, Sanmenxia, HN 472500, China



© The Author(s) 2025. **Open Access** This article is licensed under a Creative Commons Attribution-NonCommercial-NoDerivatives 4.0 International License, which permits any non-commercial use, sharing, distribution and reproduction in any medium or format, as long as you give appropriate credit to the original author(s) and the source, provide a link to the Creative Commons licence, and indicate if you modified the licensed material. You do not have permission under this licence to share adapted material derived from this article or parts of it. The images or other third party material in this article are included in the article's Creative Commons licence, unless indicated otherwise in a credit line to the material. If material is not included in the article's Creative Commons licence and your intended use is not permitted by statutory regulation or exceeds the permitted use, you will need to obtain permission directly from the copyright holder. To view a copy of this licence, visit <http://creativecommons.org/licenses/by-nc-nd/4.0/>.

## Introduction

Rhododendron is a general name of plants from *Rhododendron* L. genus from Ericaceae family. These ornamental plants are highly valued worldwide [1]. China is rich in wild rhododendron resources, with more than 600 species [2]. However, China's rich rhododendron resources have not been optimally used in urban landscape construction and economic development. One of the important reasons for the hindered development of rhododendron industry in China is poor heat resistance of rhododendron [3]. With the continuous social and economic developments, some wild plant species with small populations and little attention have been extinct or endangered due to the serious disturbance and narrow habitat [4]. *R. henanense* subsp. *lingbaoense* (*Rhl*) is a rhododendron subspecies from Henan Province, endemic to Lingbao. It is distributed in the mountaintops or ridges above 2000 m elevation in Laoyacha [5]. *Rhl* is a woody species with relatively weak natural reproduction ability. It is an ancient rhododendron tree that is a remnant of the natural forest in the Xiaoqinling Mountains [6] and has scientific research and natural heritage value as a germplasm resource bank [7].

Global temperatures have increased by approximately 1.1 °C compared to pre-industrial times [8]. Global warming has also increased the frequency of extremely hot days, seriously affecting the growth, survival and distribution of vegetation worldwide [9]. Heat stress can seriously damage the normal physiological functions of rhododendrons, which can lead to the wilting of branches and leaves or the death of plants [10]. It causes oxidative burst within cells, damaging organelles and cell membranes and leading to enzyme denaturation [11]. To cope with temperature fluctuations, plants have developed various mechanisms such as activation of signal molecules (MAPK, CDPK, etc.), antioxidant enzymes [catalase (CAT), peroxidase (POD), superoxide dismutase (SOD), glutathione peroxidase, etc.], heat shock factors (TaHSFA6e, HSF3, etc.), heat shock proteins (HSPs; HSP26, HSP17, sHSPs, etc.), starch reduction, synthesis of amino acids and proteins, and expression of many stress-related genes (ABC transporter, pyrolyte disulfide isomerase, etc.) [12, 13]. Moreover, dehydration responsive element binding proteins 1 and 2 are important transcription factors (TFs) in the regulation of drought/heat stress tolerance [14, 15]. Heat stress (HS) induces HSPs including HSP26, HSP17, and HSP70 and a complex transcription network including DREB2A and heat shock factors a1 (HSFA1s). Among them, HSFA1s is the master regulator of the HS response, which directly regulates important TFs including HSFA2, DREB2A, and HSFs [16]. Four main pathways play important roles in response to heat stress in plants; they include the heat stress factor–heat shock protein (HSF–HSP), calcium ion–calmodulin,

hormone regulation, and reactive oxygen species (ROS) [17–19].

Rhododendron plants exhibit certain heat resistance; however, most species can not withstand scorching sun and tolerate cold and humid environment. When the ambient temperature is higher than 35 °C, rhododendron plants enter dormancy; strong light causes burning and yellowing of the leaves, and the whole plant may die [20]. It was reported that with the increase of temperature, the plant height and diameter of *Rhododendron. staghorn*, *Rhododendron. rivulare* increased; the activity of SOD, contents of chlorophyll, malondialdehyde (MDA), soluble protein, and soluble sugar increased, whereas the relative water content and total biomass of leaves significantly decreased [21]. At present, high temperature in summer has become the main factor limiting the widespread application of rhododendron in urban green spaces [3].

Currently, combined metabolome and transcriptome analyses are widely used in plant research and have become a powerful tool to study the genes participating in the biosynthesis of various secondary metabolites in higher plants [22]. A previous study used metabolomic and transcriptomic analyses to assess the response of maize to high temperature stress (HTS) and revealed that the downregulation of genes encoding sucrose phosphate synthase, soluble starch synthase, and amyloclase was closely related to decreased starch content, whereas upregulation of genes encoding glutamate synthase and glutamate pyruvate transaminase led to the increase in protein content [23]. Transcriptome and metabolome analyses were performed on pitaya seedlings exposed to high temperature; 64 differentially expressed metabolites (DEMs), including sugars, organic acids, and amino acids, and 198 differentially expressed genes (DEGs) were screened. *HuPR-1* was confirmed to play a significant role in the response of pitaya to HTS [24]. Metabolome studies reported that in *Arabidopsis thaliana*, sucrose can replace proline as the main osmoprotectant of cell membrane under HTS, and the contents of proline and soluble sugar in metabolic network play a very important role in the response of plants to HTS [25]. The physiological and biochemical responses of leaves from four rhododendron varieties under HTS were studied; soluble protein content exhibited a significant downward trend with the increase of temperature, and their physiological metabolism significantly changed [26]. For example the contents of MDA, proline, reduced glutathione (GSH), superoxide dismutase (SOD), catalase (CAT), and peroxidase (POD) in *Rhl* leaves exhibited an overall trend of first increasing and then decreasing with the increasing temperature. In recent years, the studies on rhododendron are mainly focused on garden application [27], tissue culture [28], phytochemistry and pharmacology [29], drought stress, and response to cold and HS [30–32].

The molecular mechanism of response of rhododendron to high temperature has not been thoroughly studied in China and abroad. As an endangered alpine plant, *Rhl* should be studied in detail; however, studies on *Rhl* are scarce. Recently, *Rhl* genome was assembled from scratch using PacBio long-read and Illumina short-read sequencing technologies [33]. The *C2H2* gene family of *Rhl* had been identified, and its expression has been analyzed under different stress treatments [34]. The transcriptome and metabolome of *Rhl* under HTS have not been analyzed. Therefore, in this study, *Rhl* seedlings were treated at 40°C (RLH), 32°C (RLM), and 24°C (RLC), and the changes in transcriptome and metabolome were compared. The dynamic changes of the gene expression and metabolite accumulation in *Rhl* leaves at different temperatures were analyzed using RNA-seq, and liquid chromatography–tandem mass spectrometry (LC-MS/MS). qRT-PCR analysis was performed for the validation of transcriptome sequencing results. The results of this study can provide abundant genomic information for future research and help to clarify the molecular mechanisms of heat stress response of *Rhl*.

## Materials and methods

### Plant materials

In October 2023, an appropriate amount of *Rhl* seeds was collected from the Xiaoqinling National Nature Reserve in western Henan Province. *Rhl* seeds were sterilized with 2% sodium hypochlorite for 10–15 min and washed 5 times with sterile water. Further, the seeds were germinated using double filter paper method in culture dish. The seedlings were cultured under a 16 h light/8 h darkness photoperiod condition in a light incubator with the humus soil in the native territory (temperature: 24°C, light intensity: 10,000 lx, and relative humidity: 75%) until the third true leaf stage. They were divided into three groups: control group (RLC), medium temperature group (RLM), and high temperature group (RLH). The seedlings in these groups were placed at 24°C, 32°C, and 40°C in a Light incubator (Bluepard, Shanghai Yiheng Technology Co., LTD, CN), respectively, for 72 h. Further, tender leaves were collected, frozen in liquid nitrogen, and stored at -80°C. For metabolome and transcriptome analyses, six and three replicates per group were used, respectively.

### Metabolome analysis

#### Pre-processing

An appropriate amount of leaves was accurately weighed in a tube (100 mg). To this, 600 µL methanol (Fisher Scientific, Loughborough, UK) was added and vortexed for 30 s. To this, a steel ball was added. The tube was placed in a tissue grinder for 60 s at 55 Hz, followed by ultrasonication for 15 min. Further, the solution was centrifuged

at 13,400 rpm at 4 °C for 10 min, and the supernatant was filtered through a 0.22-µm membrane. The filtrate was added to the detection bottle for LC-MS.

The LC analysis was performed on a Vanquish UHPLC System (Thermo Fisher Scientific, USA). Chromatography was conducted using an ACQUITY UPLC® HSS T3 (2.1 × 100 mm, 1.8 µm; Waters, Milford, MA, USA). The column: T3, the reverse column, column temperature: 40°C. The flow rate and injection volume were set at 0.3 mL/min and 2 µL, respectively. For LC-ESI(+)-MS analysis, the mobile phases consisted of 0.1% formic acid in acetonitrile (v/v) (B2) and 0.1% formic acid in water (v/v) (A2). Gradient program was as follows: 0–1 min, 8% B2(92% A2); 1–8 min, 8–98% B2(92–2% A2); 8–10 min, 98% B2(2% A2); 10–10.1 min, 98–8% B2(2%–92% A2); 10.1–12 min, 8% B2(92% A2). For LC-ESI(-)-MS analysis, the mobile phase was acetonitrile (B3) and 5 mM ammonium formate (A3). The gradient elution procedure was the same as that for the cationic mode. MS detection of metabolites was performed on Orbitrap Exploris120 (Thermo Fisher Scientific, USA) with ESI ion source. Simultaneous MS1 and MS/MS (Full MS-ddMS2 mode, data-dependent MS/MS) acquisition was used.

### Data analysis

The original data were first converted into mzXML using MSConvert in ProteoWizard package software (v3.0.8789) [35] and further processed using R XCMS (v3.12.0) for feature detection [36]. The metabolites with relative standard deviation(RSD) > 30% in the quality control (QC) samples were filtrated. Subsequently, identification was conducted through precise MS data and matched with massbank [37], HMDB [38], and KEGG [39].

Unsupervised and supervised multivariate statistical analysis models [principal component analysis (PCA) and orthogonal partial least squares discriminant analysis (OPLS-DA), respectively] were used to differentiate the different groups using R ropls (v1.22.0) software [40]. The steps of data analysis for 6 duplicate samples in each group (RLC, RLM, and RLH) were as follows: FastQC was used for raw data quality control; Trimmomatic for trimming and filtering; STAR was used to compare the data with the reference genome; featureCounts was used to quantify gene expression; DESeq2 was used for differential expression analysis, and the false discovery rate was controlled using the Benjamini-Hochberg program. To identify the DEMs, the screening criteria were fold change ≥ 2 or ≤ 0.5, *P*-value < 0.05, and variable importance in the project (VIP) ≥ 1 [41]. The DEMs were subjected to KEGG pathway enrichment analysis using MetaboAnalyst ([www.metaboanalyst.ca](http://www.metaboanalyst.ca)) [42].

### Transcriptome sequencing analysis

The RNA-Seq of the leaves from 9 samples (RLC, RLM, and RLH) was performed by Frasergen Biotechnology Co., Ltd. (Wuhan, China). After passing the three library tests, DNA nanoballs were prepared and mounted on sequencing chips. MGISEQ-T7(PE150) sequencing platform was used for sequencing. The library preparation and quality test were performed as follows. RNA sample was extracted, and RNA quality was evaluated using NanoDrop spectrophotometer and Agilent Bioanalyzer; The cDNA library was constructed using TruSeq RNA sample preparation kit; Qubit and Agilent high sensitivity DNA kits were used for quantitative analysis and quality detection of the library. Further, SOAPnuker software (v2.1.0) was used to filter raw reads to obtain high-quality clean reads. HISAT2 software was used to compare clean data with the *Rhl* reference genome [33], and alignment quality was assessed using RSeQC (v3.0.1). For the known genes, QC, database annotation, quantitative expression, analysis of significant difference ( $P$ -value < 0.05), GO and KEGG functional enrichment analyses, mining of DEGs, and TF expression analysis were conducted. GO and KEGG enrichment analyses were conducted using Fisher's exact test, and core genes within the GO/KEGG annotated gene set were identified using GSEA (Gene Set Enrichment Analysis, <http://gsea-msigdb.org/gsea/>). For NR (NCBI non-redundant protein sequence), PFAM (protein family), and SWISSPROT (manually annotated and reviewed protein sequence database) annotations, a homology based approach was applied. BLAST was used for sequence comparison with the NR database. (<https://blast.ncbi.nlm.nih.gov/Blast.cgi>). InterProScan was used to identify protein domains and functional sites, which aid in PFAM annotation(<https://www.ebi.ac.uk/interpro/about/interproscan/>). HMMER was used to search protein sequences in the PFAM database. (<http://hmmer.org/>). UniProt was used to access SWISSPROT data and perform homology-based annotations(<https://www.uniprot.org/>). TFs were predicted using PlantTFDB 4.0. DESeq2 was used for the analysis of DEGs from each group of replicated samples. The analysis included standardization of counting data and Estimated dispersion. The DEGs were identified based on adjusted thresholds of  $P$  < 0.05 and  $\log_2$  fold change > 1. These steps ensured the robustness and reliability of the results, providing a clear understanding of the differences in gene expression between the groups.

### Combined transcriptome and metabolome analyses

Through KEGG pathway enrichment analysis(<https://www.kegg.jp>), the DEGs and DEMs were annotated to multiple metabolic pathways, and relevant metabolic pathways were screened and analyzed. In addition, R software was used to calculate the Pearson's correlation coefficient

of DEGs and DEMs and create the correlation heatmap. The DEGs and DEMs with  $P$ -value < 0.05 were selected to draw the network map using R version 3.5.1 software. The original transcriptome sequencing data have been submitted to the NCBI BioProject database with login number: PRJNA1141191.

### Quantitative real-time PCR (qRT-PCR) analysis

Total RNA was isolated using a Plant magnetic bead RNA extraction kit (Lingjun Biotechnology Inc., Shanghai, China). RNA concentration and purity were assessed using a NanoDrop-2000 (Thermo Fisher Scientific Inc., Waltham, USA). The first-strand cDNA was synthesized using Rever Tra™ kit (TOYOBO, Shiga, Japan), with 2  $\mu$ g total RNA(DNA contamination had been removed), as per the manufacturer's protocol. qRT-PCR analysis was performed using the CFX96™ real-time detection system (Bio-Rad Laboratories, Inc., Hercules, USA). All reactions were performed using the Bestar™ qPCR Master-Mix according to the manufacturer's protocol (Cat. No. 2026789, DBI, DE), with three biological and three technical replicates for each sample. The primers of 9 genes and internal reference gene *EF1 $\alpha$*  are given in Table S1. The expression was calculated using  $2^{-\Delta\Delta CT}$  method. SPSS 13.0 was used to analyze the results using ANOVA.

## Results

### Metabolome analysis

#### Sample quality control (QC) and data analysis

PCA was performed using the datasets obtained from the RLC, RLM, and RLH samples. The results indicated that the metabolites from three groups of samples treated at different temperatures were clearly separated in the score map, where the first principal component (PC1) and the second principal component (PC2) were separately plotted. For ESI<sup>+</sup> models, PC1 and PC2 accounted for 18.4% and 9.8% of the total change, respectively. For ESI<sup>-</sup> models, PC1 and PC2 accounted for 17.2% and 9.8% of the total change, respectively (Fig. 1A and B). The positions of the three sample points on the PCA were relatively far, indicating significant differences among them. The QC samples were tightly clustered and located near the center of all samples, indicating good reproducibility of the experiment. The OPLS-DA plots were used to model the DEMs among RLC, RLM, and RLH. This model is stable and reliable and can be used to screen DEMs. At each temperature, both ESI modes could effectively separate the RLC, RLM, and RLH samples (Fig. 1C and D). These results indicated significant differences among the three treatments.

#### Analysis of differentially expressed metabolites (DEMs)

A total of 78 DEMs were screened among the three treatments (Table S2) with the criteria VIP value > 1 and



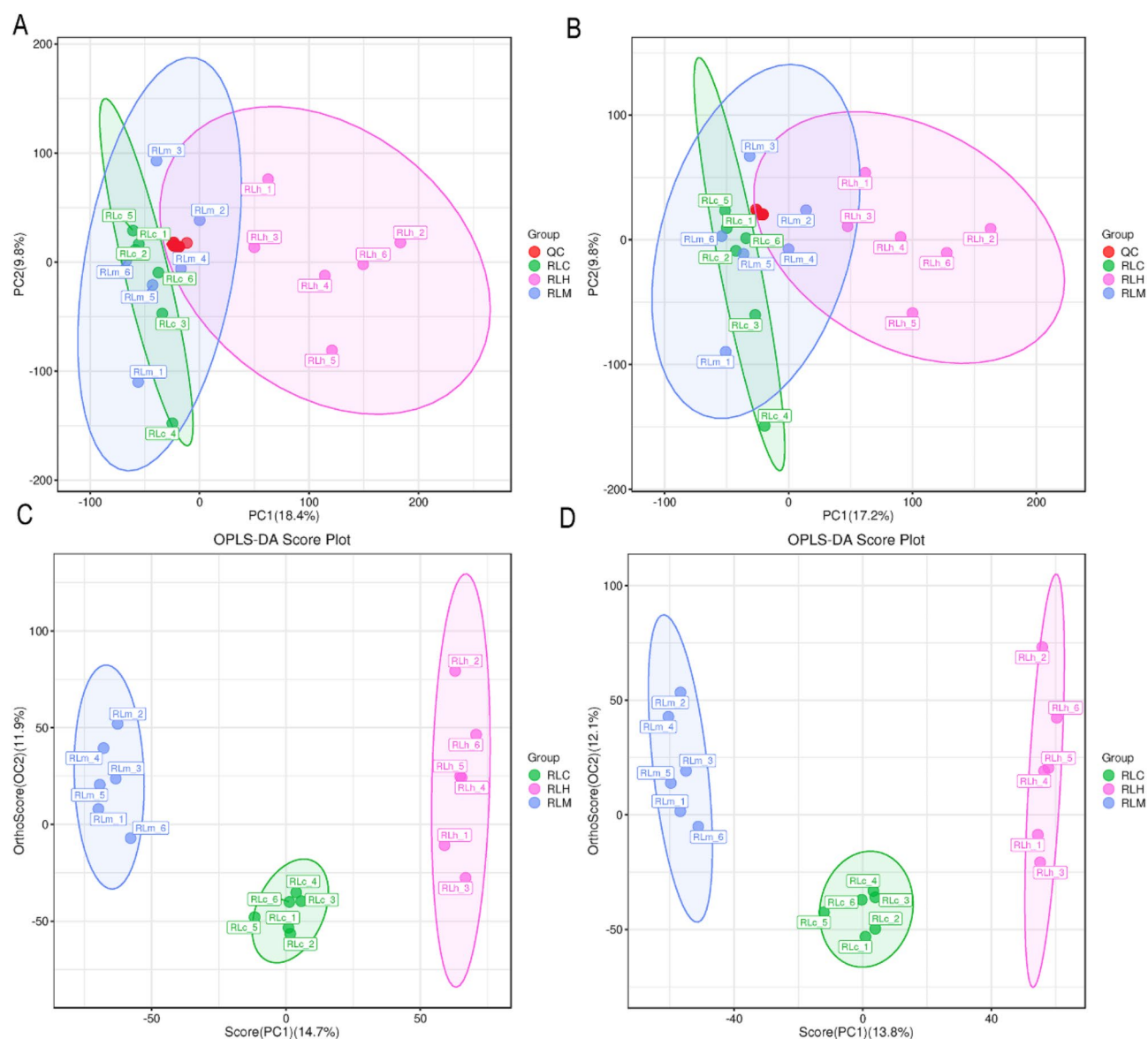


**Fig. 1** Principal component analysis (PCA) (QC sample) and orthogonal partial least squares discriminant analysis (OPLS-DA) scores of RLH group versus RLM group versus RLC group (A and C) Positive ion models. (B and D) Negative ion models

$P$ -value  $< 0.05$ . The DEMs were mainly distributed in fatty acyls group (12.8%), benzene and substituted derivatives (10.3%), carboxylic acids and derivatives (10.3%), and others (23.1%). A total of 76 DEMs were detected by comparing RLH vs. RLC (Fig. 2A). Among them, 40 and 36 DEMs exhibited increased and decreased levels, respectively; they included some amino acids namely L-proline, isoleucine, leucine, ornithine, methionine, and histidine (Fig. 2A, C). In RLM vs. RLC, the increase in amino acids content was insignificant. However, in RLH vs. RLC, it was significant by 2.11–5.33 times, indicating that HTS significantly increased the content of amino acids.

In total, 90 DEMs were detected in RLH vs. RLM. Among them, 33 and 57 exhibited increased and decreased levels, respectively (Fig. 2A and D). Overall, 43 DEMs were detected in RLM vs. RLC. Among them, 29 and 14 exhibited increased and decreased levels, respectively (Fig. 2A and E). In conclusion, the alterations in the metabolites in RLH vs. RLM and RLH vs. RLC were greater than those in RLM vs. RLC, and the metabolite content of *Rhl* under HTS(40°C) was significantly different compared with that under 35°C and 24°C (Fig. 2C-E).

RLH vs. RLC, RLH vs. RLM, and RLM vs. RLC had 27, 25, and 15 unique DEMs, respectively (Fig. 2B). Among the unique DEMs in RLM vs. RLC, the contents of L-rhamnono-1,4-lactone, (-)-bornesitol, and

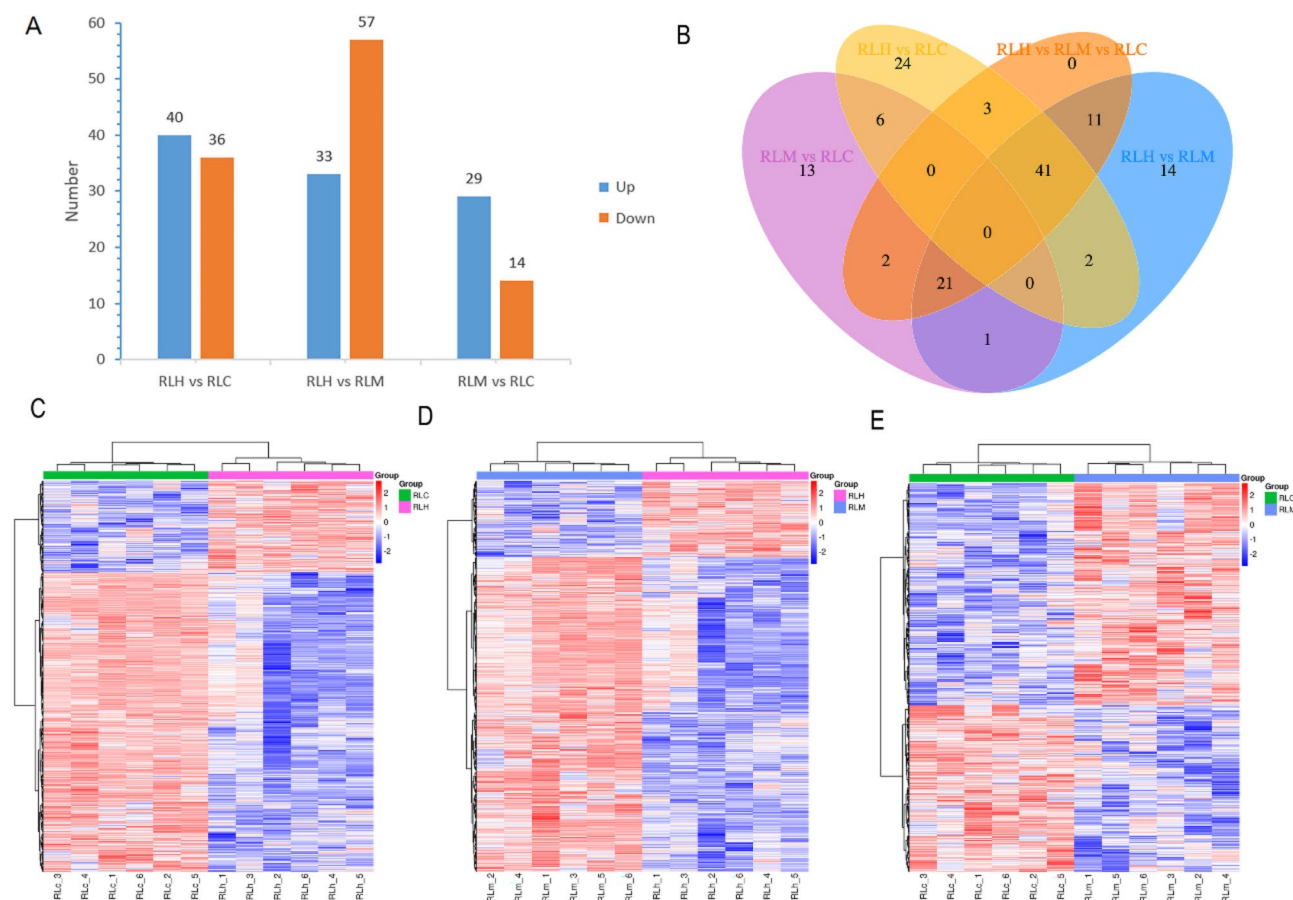


**Fig. 2** The differentially expressed metabolites (DEMs) among three comparison. **(A)** The DEMs of up- (orange) and down-regulated (blue) metabolites in different comparison. **(B)** Venn diagram of DEMs. **(C, D and E)** Heatmap of DEMs. The complete linkage hierarchical cluster analysis (HCA) method was applied to reflect the normalized metabolite content in each sample, which is represented by a single row with ranging color chroma from red (high abundance) to blue (low abundance). **C:** RLC vs. RLH; **D:** RLH vs. RLM; **E:** RLC vs. RLM

6-hydroxyhexanoic acid were significantly increased by 3.12–3.99 times (Tables S3–S5;  $P$ -value < 0.05). Among the unique DEMs in RLH vs. RLC, the contents of L-methionine, D-ornithine, isoquercetin, cyclic guanosine phosphate, and quercetin were significantly increased by 3.11–6.62 times ( $P$ -value < 0.05). Among the unique DEMs in RLH vs. RLM, the contents of 2-deoxystreptamine, 3-methyl-L-tyrosine, and bovinic acid were significantly increased by 2.21–2.64 times ( $P$ -value < 0.05).

#### KEGG pathway enrichment analysis

In RLH vs. RLC, 76 DEMs were annotated to 50 pathways. Among them, the significantly enriched metabolic pathways were flavone and flavonol biosynthesis, D-amino acid and ABC transporters transport, and others (Fig. 3A). In RLH vs. RLM, 90 DEMs were enriched in 56 metabolic pathways. Among them, the significantly enriched metabolic pathways were linoleic acid metabolism, flavonoid and flavonol biosynthesis, tyrosine metabolism, ABC transport, and other pathways

(Fig. 3B). In RLM vs. RLC, 43 DEMs were annotated to 29 metabolic pathways (Fig. 3C). Among the above pathways, the DEMs enriched in D-amino acid metabolism and ABC transporter pathway were more in number, and their  $P$ -values were relatively small. The impact value of flavonoid and flavonol biosynthesis pathway was larger (Fig. 3).

Among the DEMs with increased expression in RLH vs. RLC, two (quercetin and isoquercetin) were involved in flavonoid and flavonol biosynthesis pathway, and isoquercetin was the unique DEM (Fig. S1A). Six DEMs (ornithine, L-leucine, L-histidine, L-proline, mannitol, and L-isoleucine) were involved in the D-amino acid metabolic pathway, among which L-methionine, D-ornithine, and cis-4-hydroxy-d-proline were the unique DEMs (Fig. S1B). The results indicated that D-amino acid metabolism and flavonoid and flavonol biosynthesis pathway are affected under HTS, resulting in the upregulation of metabolites. The DEMs enriched in ABC transporter pathway mainly included phosphate and amino acid transporters, exhibited increased expression (Fig.

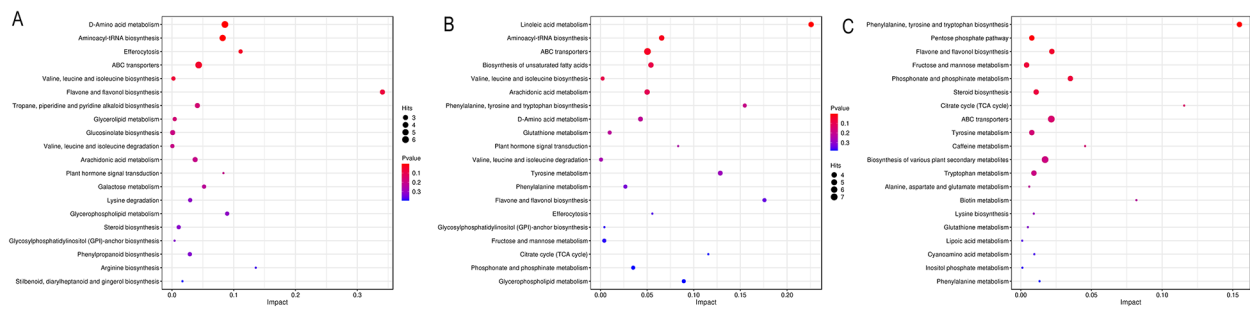


**Fig. 3** KEGG pathway enrichment analysis of DEGs in *R. henanense* subsp. *lingbaoense* after various temperature treatments (A) RLH vs. RLC. (B) RLH vs. RLM. (C) RLM vs. RLC. The dot color represents the *P*-value; the redder it is, the more significant the enrichment. The size of the dots represents the number of differential metabolites enriched in the pathway

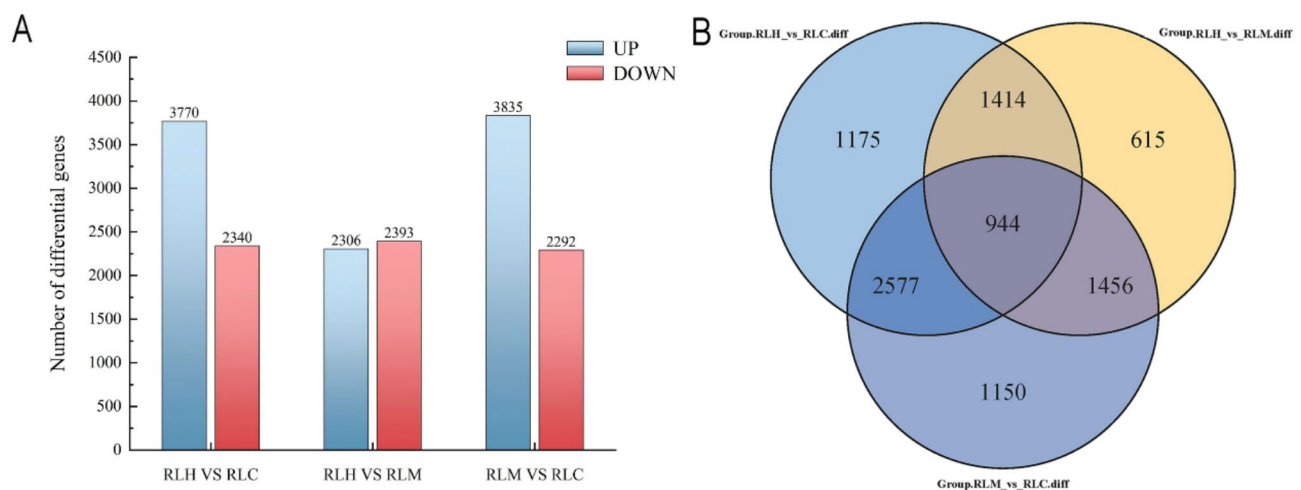


**Fig. 4** The differentially expressed genes (DEGs) among three comparison. (A) The DEGs of up- (red) and down-regulated (blue) genes in different comparison. (B) Venn diagram of DEGs. 3.2.3. Analysis of DEGs

S1C). ABC transporter pathway is an important pathway for cell transport and may be an important pathway in the response of *Rhl* seedlings to HTS.

### Transcriptome analysis

#### Quality evaluation

A total of 66.798 Gb clean data (after QC) was obtained, and the average amount of clean data of each sample was 7.422 Gb. The percentage of Q30 bases was >95.38%, and the GC content was 45.76–46.16% (Table S6). The results of 18,110, 10,157, 26,314, 20,932, 358, and 18,480 genes have been successfully noted on the GO, KEGG, NR, PFAM, STRING, and SWISSPROT databases, respectively.

#### Detection of differentially expressed genes (DEGs)

In total, 8450 DEGs were identified by comparison, of which 6110 DEGs were detected in RLH vs. RLC (3770 upregulated and 2340 downregulated); 4429 DEGs were identified in RLH vs. RLM (2306 up-regulated and 2393 down-regulated); and 6127 DEGs (3835 upregulated and

2292 downregulated) were detected in RLM vs. RLC (Fig. 4A). Venn diagrams were drawn for the DEGs in the three comparison groups, with 944 co-expressed genes (Fig. 4B). These results indicated that the expression levels of these DEGs may change during HTS.

KEGG pathway enrichment analysis was performed on the DEGs (Fig. 5A-C). In RLH vs. RLC, DEGs were majorly enriched in photosynthesis, secondary metabolite biosynthesis, carbon metabolism, flavonoid biosynthesis, metabolic pathways, and other pathways. Significantly enriched pathways for the DEGs in RLH vs. RLM included metabolic pathways ( $P$ -value < 0.001), secondary metabolic biosynthesis ( $P$ -value < 0.001), plant hormone signal transduction ( $P$ -value < 0.001), etc. The enriched pathways for the DEGs in RLM vs. RLC mainly included metabolic pathway, signal pathway, carbon metabolism, secondary metabolic biosynthesis, plant hormone signal transduction, flavonoid biosynthesis, etc. These pathways in *Rhl* may be important in resisting HTS. GO pathway enrichment analysis revealed that 4095, 684, and 1724 genes were significantly enriched

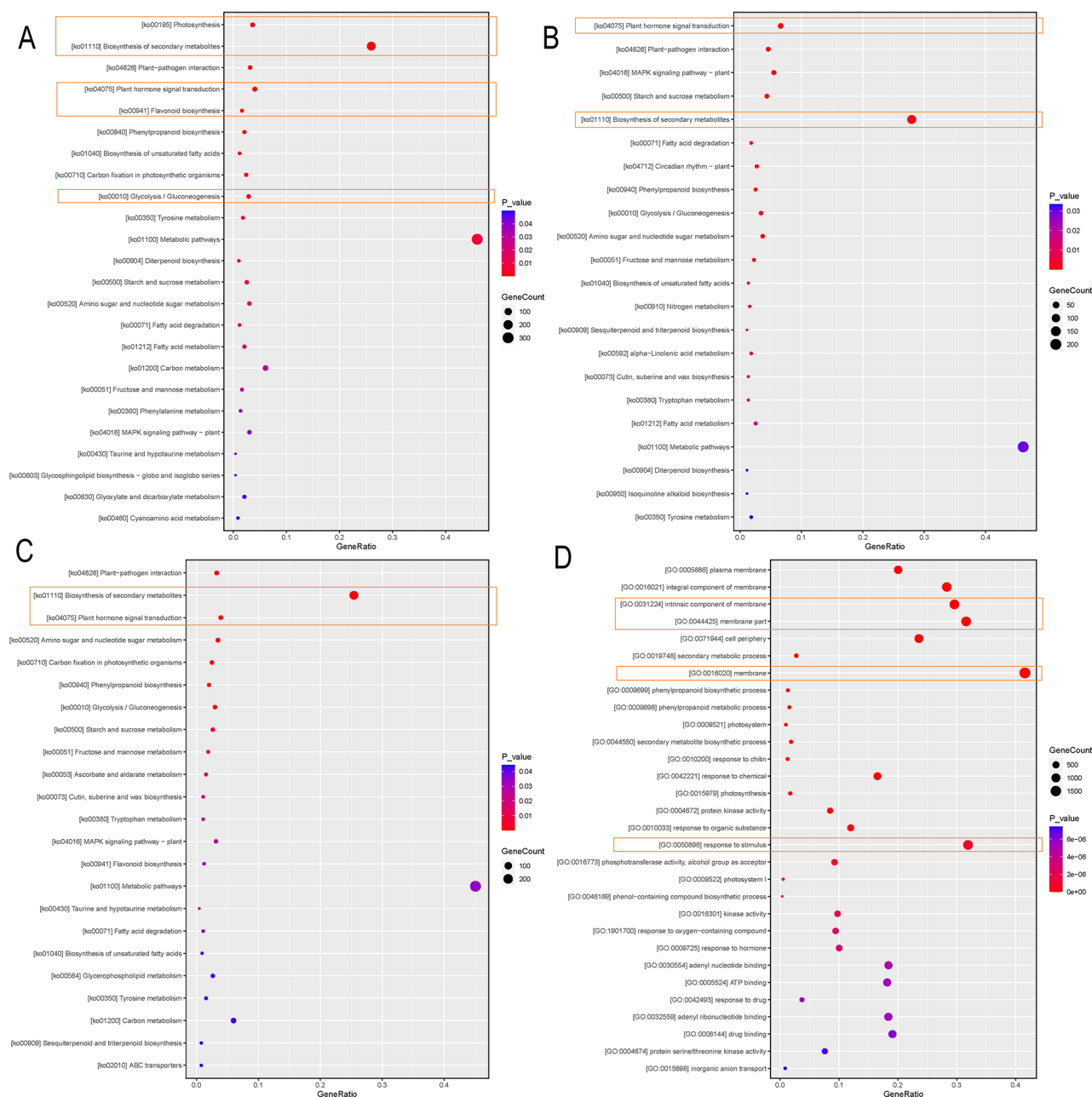


**Fig. 5** KEGG and GO pathway enrichment analyses of DEGs in *Rhl*. KEGG pathway enrichment analysis of DEGs in **(A)** RLH vs. RLC. **(B)** RLH vs. RLM. **(C)** RLM vs. RLC. GO pathway enrichment analysis of DEGs in **(D)** RLH vs. RLC. The dot color represents the *P*-value; the redder it is, the more significant the enrichment. The size of the dots represents the number of differential genes enriched in the pathway

in biological process (BP), cell composition (CC), and molecular function (MF), respectively (Fig. S2). The most genes (1753) were enriched in Membrane (Fig. 5D). Moreover, 1346, 1334, 1249, and 1195 genes were mainly enriched in stimulus, membrane part, membrane intrinsic component, and membrane integral component, respectively.

### Mining of DEGs

GO pathway enrichment analysis of DEGs in RLH vs. RLC revealed that several genes were enriched in the response to stimulus pathway in Biological process (BP), from which genes related to oxidative stress and HS were screened (Fig. S2). KEGG pathway enrichment analysis revealed that photosynthesis and secondary metabolite biosynthesis were the significantly enriched pathways. Glycolysis/gluconeogenesis pathway can provide glucose for photosynthesis for secondary photochemical reaction.



Analysis of the genes associated with these three pathways can help to reveal the mechanism of response of *Rhl* to HTS (Fig. 5A).

#### DEGs related to glutathione-S-transferase (GST)

Under HTS, plants produce excessive ROS, and antioxidant enzymes play an important role in removing harmful ROS. Glutathione-S-transferase (GST) is a class of antioxidant enzymes involved in the metabolic pathway of glutathione and can play a role in protecting organisms from high temperatures. Overall, 13 genes related to GST were screened from the DEGs (Table S7). Under HTS, except *Rhe005696* and *Rhe017231*, the other 11 genes were upregulated.

#### DEGs related to HS response and photosynthesis

Under HS, HSPs are produced to protect plants. In RLH and RLC, 43 DEGs were related to HSP (Table S8), of which 35 were significantly downregulated and 8 were significantly upregulated. These results suggested that *Rhl* may inhibit the expression of genes encoding HSPs for self-protection in high temperature environments. It might be due to the tolerance of the plant to high temperatures. Photosynthesis is more sensitive to temperature. Compared with RLC, all 31 significant DEGs related to photosynthesis in RLH were upregulated (Table S9).

#### Genes related to secondary metabolites and Glycolysis/gluconeogenic biosynthesis

Various secondary metabolites produced by secondary metabolic pathways help plants in coping with adverse environments. The top five genes with the most

significant upregulation (328 in total) were selected (Table S10). The most significantly upregulated gene was *Rhe001827* encoding chalcone and stilbene synthases that affect the production of flavonoids, which not only have antioxidant properties but also protect plants from heat damage. Second, an antioxidant enzyme POD encoded by *Rhe016769* is an oxidoreductase in plant tissues and organs; it can eliminate hydrogen peroxide accumulated in the body and protect plants [13]. *Rhe005479* and *Rhe012217* encode terpene synthase (TPS), and catalytic production of terpene compounds by them plays a significant role in plant stress tolerance [43]. Glycolysis/ gluconeogenesis is closely related to photosynthesis. Overall, 40 DEGs related to glycolysis/gluconeogenesis were analyzed, most of which were significantly upregulated. The top five are shown in Table S11.

#### Transcription factor (TF) expression analysis

To investigate the expression of TFs in *Rhl* after HTS, stress-related TF family members such as bHLH, HSF, bZIP, ARF, NAC, MYB, AP2/ERF, WRKY, and C2H2 were analyzed. Overall, 3, 10, 17, 9, 2, 65, 50, 32, and 12 genes of bHLH, HSF, bZIP, ARF, NAC, MYB, AP2/ERF, WRKY, and C2H2 families were screened, respectively. The heatmap of these TF families (Fig. 6) revealed that compared with RLC, most members of bHLH, bZIP, ARF, NAC, MYB, AP2/ERF, and WRKY TF families were upregulated in RLM and RLH, which may be the reason for the higher number of upregulated genes in different comparison groups (RLH vs. RLC, RLH vs. RLM, and RLM vs. RLC). Moreover, it was observed that some members of the WRKY and AP2 families were upregulated under

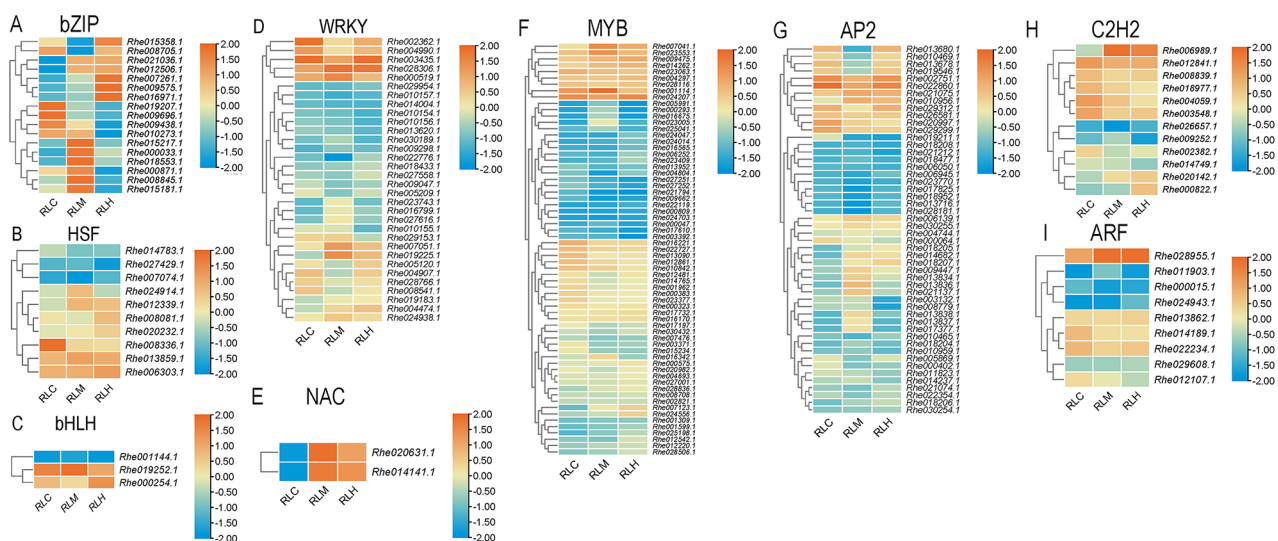


**Fig. 6** Heatmap of differentially expressed *Rhl* transcription factors in the transcriptome. **(A)** Heatmap of 17 differentially expressed bZIP TFs. **(B)** 10 differentially expressed HSF TFs. **(C)** 3 differentially expressed bHLH TFs. **(D)** 32 differentially expressed WRKY TFs. **(E)** 2 differentially expressed NAC TFs. **(F)** 65 differentially expressed MYB TFs, **(G)** 50 differentially expressed AP2 TFs. **(H)** 12 differentially expressed C2H2 TFs. **(I)** 9 differentially expressed ARF TFs. Orange indicates high expression, and blue indicates low expression

moderate heat stress (RLM), but downregulated under high heat stress (RLH). The TFs directly related to heat stress were *Rhe007074* (HSFB4), *Rhe012339* (HSFB3), and *Rhe020232* (HSFAB). They were significantly upregulated in RLM vs. RLC and RLH vs. RLC. *Rhe013859* (HSB2A) had the highest expression levels in RLM, and *Rhe008336* (HSF30) and *Rhe006303* (HFA4B) were significantly downregulated (See supplementary material1). These results demonstrated that complex transcriptional networks associated with heat shock response (HSR) are composed of many TF families.

### Combined transcriptome and metabolome analyses

Combined analysis of DEMs and DEGs among different samples was conducted. In RLH vs. RLC, RLH vs. RLM, and RLM vs. RLC, 45, 48, and 27 DEM and DEG co-annotation pathways were observed (Supplement material2-1-3). In three comparison groups, 13 distinct enrichment pathways of DEMs and DEGs were noted (Supplement material2-4). These results indicated that HTS may induce changes in the metabolites of these pathways. The flavonoid biosynthesis pathway and ABC transport pathway closely related to HTS were selected for in-depth analysis.

### Flavonoid biosynthesis pathway in RLH vs. RLC

Both transcriptome and metabolome analyses in this study indicated a significant upregulation of metabolites from flavonoid biosynthesis pathway. Therefore, the expression of genes and metabolites related to flavonoid biosynthesis under HTS was further investigated. Compared with RLC, the expression level of *Rhe002465*, *Rhe006335*, *Rhe014544*, *Rhe011722*, *Rhe014879*, *Rhe016929*, *Rhe019664*, *Rhe019800*, *Rhe024744*, *Rhe025440*, *Rhe025485*, *Rhe026310*, and *Rhe001827* was significantly increased, whereas that of *Rhe006334*, *Rhe022609*, and *Rhe002395* was significantly decreased in RLH (Fig. 7A). Compared with RLC, quercetin content was higher and kaempferol content was lowered in RLH (Fig. 7B). The correlation between DEGs and DEMs revealed that kaempferol was positively correlated with *Rhe002395* and *Rhe022609* (correlation coefficients: 0.6761 and 0.8052, respectively,  $P$ -value < 0.001). Conversely, quercetin was negatively correlated with them (Fig. 7C and D).

p-Coumaroyl-CoA is catalyzed by CHS to form chalcone, followed by CHI to form naringen, F3H to form dihydrokaempferol, FLS to form kaempferol, F3H to form dihydroquercetin, and finally FLS to form quercetin (Fig. 8). High temperature induced significant upregulation of CHS, E5.5.1.6, and F3H, the three synthetases in the flavonoid biosynthesis pathway (the significantly upregulated regulatory genes of three enzymes are given in Fig. 8) and further induced significant accumulation

of quercetin. In conclusion, high temperature decreased kaempferol but promoted quercetin synthesis, thereby enhancing the stress tolerance of *Rhl* under HTS.

### ABC transport metabolic pathways in RLH vs. RLC

In RLH vs. RLC, 7 DEGs and 6 DEMs were identified in the ABC transport pathway. The 7 DEGs belong to the ABC transporter A3, ABCB1, and ABCC10 subfamilies, respectively (Table S12). Analysis of DEGs revealed that compared with RLC, the expression of *Rhe007348*, *Rhe018087*, *Rhe021651*, and *Rhe021648* was significantly increased, whereas that of *Rhe012338*, *Rhe023749*, and *Rhe029044* was significantly decreased in RLH (Fig. 9A, Table S12). DEM abundance analysis revealed that compared with RLC, L-isoleucine, L-leucine, L-proline, and ornithine levels significantly increased ( $P$ -value < 0.05), and mannitol levels decreased in RLH (Fig. 9B). *Rhe007348* was not highly correlated with other metabolites except mannitol. The remaining genes were highly correlated with DEMs in the ABC transport pathway. *Rhe018087*, *Rhe021648*, and *Rhe021651* were negatively correlated with mannitol but positively correlated with other metabolites (Fig. 9C and D).

### qRT-PCR analysis for the validation of transcriptome sequencing results

To further verify the reliability of transcriptome data, nine genes (*Rhe000027*, *Rhe002895*, *Rhe004212*, *Rhe007247*, *Rhe012415*, *Rhe012485*, *Rhe013826*, *Rhe015229*, and *Rhe023454*) were randomly selected from 944 DEGs among the three comparison groups for qRT-PCR analysis, and the correlation coefficients were all greater than 0.84 (Table S13). The results of qRT-PCR were consistent with the trend of transcriptome sequencing results, indicating the reliability of RNA-seq data. (Fig. 10).

## Discussion

### Heat stress increases metabolism of amino acids and flavonoids in *Rhl*

In the field of Chinese medicine, rhododendron is one of the research hotspots. It has rich chemical composition and mainly contains volatile oil, diterpene, triterpene, sesquiterpene, steroid, alkanes and their oxygen-containing derivatives, alcohols, flavonoids, and coumarins [44, 45]. *R. irroratum* and *R. decorum* have medicinal value [46, 47]. Flowers of *R. decorum* can be used as food in local folk customs [48]. It was reported that total flavonoids in *R. argentea* extract had a certain therapeutic effect in ischemic heart disease [49]. In this study, 78 DEMs were detected in *Rhl* after HTS; they were enriched in fatty acyl groups, carboxylic acids and their derivatives, isoprene lipids, benzene and its substituted derivatives, organic oxygen compounds, terpene lactones, and

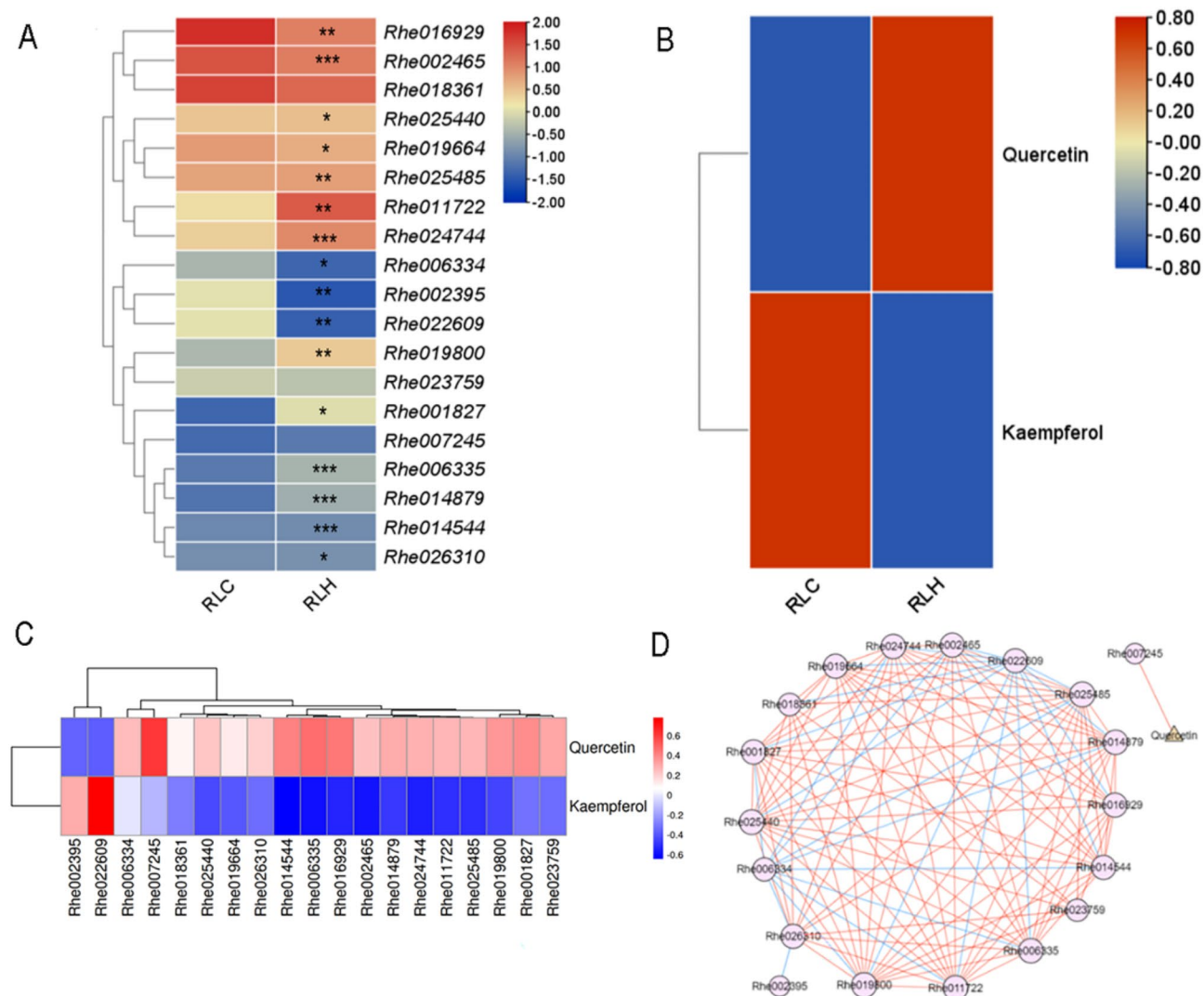


**Fig. 7** Correlation analysis of Flavonoid biosynthesis pathway between transcriptome and metabolic group in *Rhl* high temperature (RLH) and control group (RLC). **(A)** Flavonoid biosynthesis pathway related DEGs analysis. **(B)** Differential metabolite expression pattern analysis. **(C and D)** Analysis of correlation between DEGs and DEMs. Note: **(A, B, and C)** \*:  $P < 0.05$ ; \*\*:  $P < 0.01$ ; \*\*\*:  $P < 0.001$ . **(D)** Correlation coefficient  $> 0.8$ . Orange or red indicates high expression, and blue indicates low expression

phenols (Table S2). Considering these metabolites in *Rhl*, it may have significant medicinal value.

Plants respond to HTS through a series of intracellular metabolic reactions, such as starch production, amino acid and protein syntheses, and production of abscisic acid, antioxidants, and other protective molecules [50, 51]. In this study, *Rhl* accumulated several amino acids and their derivatives including proline, histidine, and leucine, which can be used as osmotic protectants and molecular chaperones. Moreover, they play an important role in eliminating ROS, stabilizing the protein structure, and maintaining intracellular homeostasis [52] (Table. 2). Therefore, accumulation of amino acids and upregulation of related metabolic pathways are important ways for plants to cope with stress. KEGG pathway enrichment

analysis revealed that the D-amino acid metabolism pathway promoted the expression of methionine, ornithine, proline, etc., whereas the ABC transporter pathway increased the transport of phosphate and amino acids. This demonstrated that amino acid metabolism and expression of corresponding amino acids were important pathways for *Rhl* to respond to high temperature. This was consistent with a study reporting that *Spinacia oleracea* promoted amino acid metabolism under HTS [53]. Another important enriched KEGG pathway was flavonoid and flavonol biosynthesis. Flavonoid compounds are rich in hydroxyl groups and have antioxidant effects; for example, phenolic hydroxyl groups in quercetin and isoquercetin provide hydrogen atoms to react with free radicals [54]. In this study, the unique flavonoid DEMs

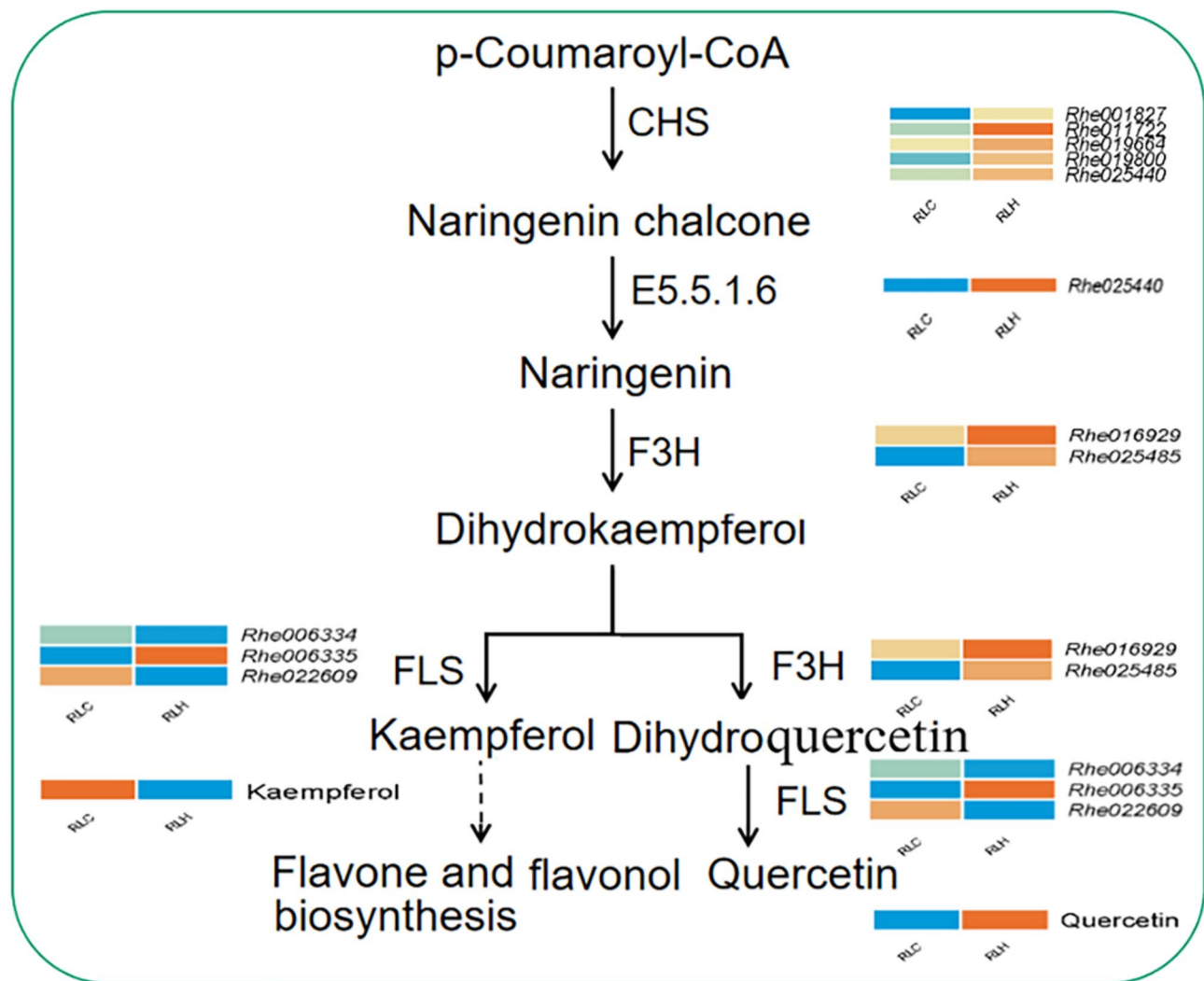


**Fig. 8** Flavonoid biosynthesis pathway in *R. henanense* subsp. *Lingbaoense*. The heatmaps were drawn according to the FPKM values from the transcriptome datasets. Columns and rows in the heatmap represent samples and genes, respectively. The color scale indicates fold changes (Log2) in gene expression. chalcone synthase (CHS), flavanone 3-hydroxylase (F3H), flavonol synthase (FLS)

in RLH vs. RLC were the most abundant, among which quercetin and isoquercetin were upregulated after HTS. This indicated that flavonoids play an important role in the tolerance of *Rhl* to HTS.

#### Expression analysis of key genes and transcription factors related to heat stress in *Rhl*

In this study, after RNA-seq of *Rhl* samples, 94,451 genes were obtained and annotated, which were close to the previously reported data of *R. hainanense*, *R. molle*, and *R. irroratum* [55, 56]. Overall, 8450 DEGs were identified in three comparison groups. 9 genes were randomly selected to validate the reliability of RNA-seq results using qRT-PCR (Fig. 2) [57]. The results suggested that heat stimuli significantly affected the transcriptome profiles in *Rhl* and provided more meaningful information for further studies on heat tolerance in rhododendron.

GO pathway enrichment analysis revealed that the DEGs were enriched in response to heat, membrane, response to stimulus, ROS, and abiotic stimuli, which were the top enriched GO terms in RLH vs. RLC (Fig. 5D). KEGG pathway enrichment analysis revealed that 1116 DEGs were significantly enriched in biosynthesis of secondary metabolites, flavonoid biosynthesis, plant hormone signal transduction, glycolysis/ gluconeogenesis, etc. (Fig. 5A–C). These results indicated that signal pathways related to HS were multiple and complex in *Rhl*, which is consistent with model plants such as *Arabidopsis* and rice [58, 59]. These results were important for providing reference resources for molecular research in rhododendron plants in the future.

High temperature can damage plant cell membrane system [60]. GO pathway enrichment analysis revealed that the number of genes enriched in membrane was the



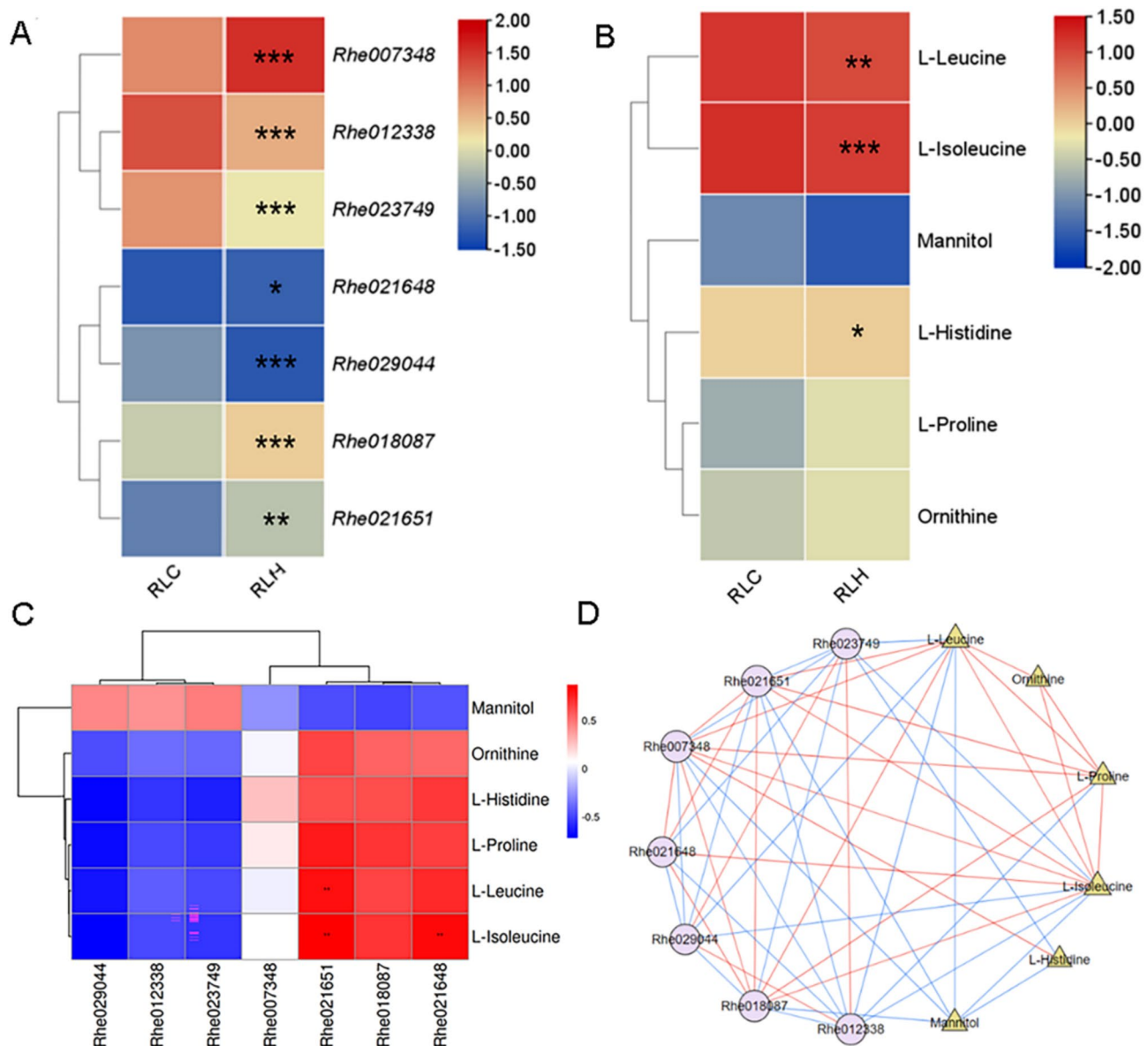


**Fig. 9** Correlation analysis transcriptome and metabolome data of ABC metabolic pathway in *Rhl* between group high temperature (RLH) and control (RLC) groups. **(A)** Relevant DEMs. **(B)** DEM expression. **(C and D)** Analysis of correlation between DEGs and DEMs. Note: **(A, B, and C)** \*:  $P < 0.05$ ; \*\*:  $P < 0.01$ ; \*\*\*:  $P < 0.001$ ; **(D)** Correlation coefficient  $> 0.8$ . Red or orange color indicates high expression, and blue color indicates low expression

highest. It could be predicted that the response of *Rhl* to HTS was through its influence on the cell membrane. HS can stimulate ROS production because it increases the levels of superoxide anion ( $O_2^-$ ), hydroxyl radical ( $HO\cdot$ ), and hydrogen peroxide ( $H_2O_2$ ) in the mitochondria [61, 62]. Excessive accumulation of these oxygen radicals results in cellular damage and death [63]. However, plants have evolved mechanisms to balance the production and scavenging of ROS through enzymatic and nonenzymatic antioxidative processes [63]. High antioxidant capacity, such as that obtained by enhancing the activities of SOD, POD, CAT, ascorbate peroxidase, and glutathione reductase, is conducive to improving the heat tolerance

of plants [64, 65]. In this study, 11 genes related to GST were screened for upregulation. *Rhe016769* encoding POD was significantly upregulated. It is speculated that the high antioxidant capacity acquired by enhancing the activity of GST and POD is beneficial for eliminating ROS and improving heat tolerance in *Rhl*.

The heat tolerance of rhododendron is mainly regulated by the physiological function of the photosynthetic system [66]. Photosynthesis is very sensitive to temperature. In this study, 31 genes related to photosynthesis were significantly upregulated, indicating that high temperature improves photosynthesis in *Rhl*. Under stress conditions, the ability of plants to absorb and utilize

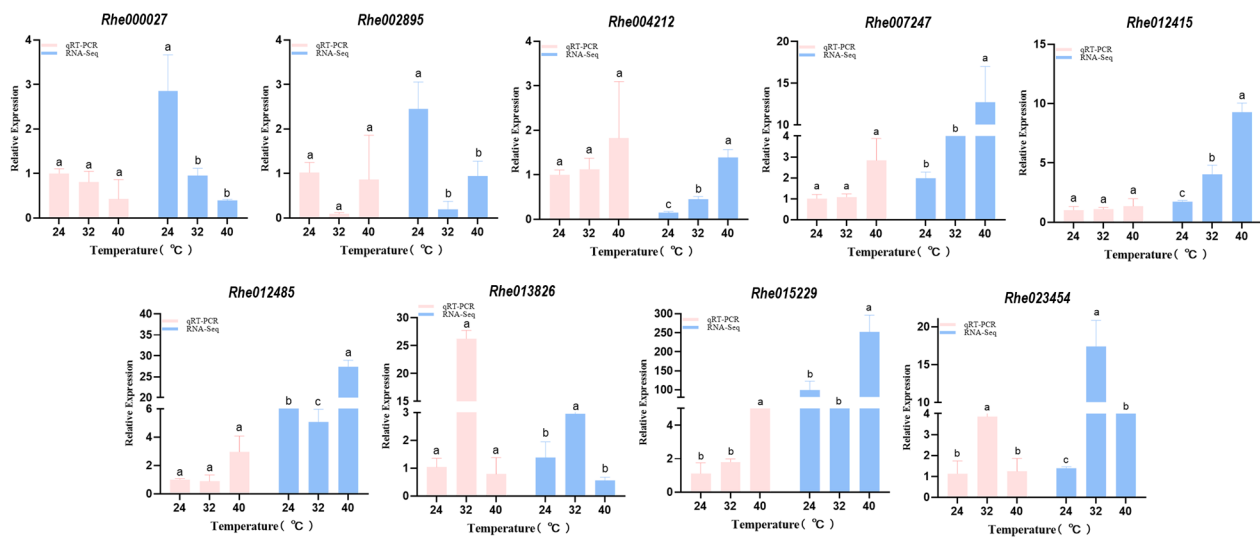


**Fig. 10** Verification of transcriptome results using qRT-PCR. Note: Different letters indicate significant differences in different temperature groups ( $P$ -value < 0.05)

light energy is greatly reduced, resulting in increased light inhibition [67]. Under HTS, several protein subunits in the light and electron transport chains (such as Psb27 and Psb28) and coenzymes (such as CP43) mediate PSII repair [68, 69]. In this study, photosynthesis-related genes were upregulated. This could be because photosynthesis in *Rhl* was improved under HTS, or photosynthesis-related genes were downregulated and photosynthesis was inhibited at first [70]. Further, with the increased duration of stress, Psb28 and other mediated PSII repair, and the photosynthesis-related genes were upregulated. However, this should be further studied and verified. Furthermore, photosynthesis is closely related to glycolysis/gluconeogenesis, which can provide glucose for secondary photochemical reactions. This pathway can be used as a protective mechanism of cells under HTS [71]. Most genes regulating glycolysis/gluconeogenesis-related proteins were significantly upregulated, and the regulation of these genes, photosynthesis related genes, antioxidant related genes, and HSP-related genes may alleviate HTS-induced damage to *Rhl*.

HSP accumulation can enhance the heat tolerance of plants [72]. HSP90 plays a protective role in heat shock reaction [73]. HSP70 family proteins are expressed under stresses such as high temperature, cold, and stimulation by chemical reagents [74]. Similarly, it was reported that with an increase in temperature, stress-associated genes including *CfAPX1*, *CfAPX2*, *CfHSP11*, *CfHSP21*, *CfHSP70*, *CfHSE1a*, and *CfHSEB4* were upregulated in *Cryptomeria fortunei* under HTS [75]. In this study, highly enriched HSPs were mostly downregulated under HTS (Table S8) probably because of considerable difference between the high temperature to which the plants were exposed and optimal growth temperature. After the

gene expression reached the maximum value, it exhibited a downward trend because of its intolerance to excessive temperature [76]. It is always believed that HSPs can protect plants from damage. In this study, 35/43 DEGs related to HSP were significantly downregulated. *Rhl* may inhibit the expression of genes encoding HSPs for self-protection under high temperature environments, but further research is needed. It was concluded that flavonoids can help rice plants to resist high temperature and heat damage [77]. Significant upregulation of chalcone synthase encoded by *Rhe001827* would increase the yield of flavonoids and enhance the tolerance of *Rhl* to high temperature. This suggested that flavonoid biosynthesis is also an important pathway in *Rhl* in response to HTS, which is consistent with the metabolome analysis. This enhanced the understanding of molecular mechanism of response of *Rhl* to high temperature.

TFs directly regulate the expression levels of stress-responsive genes and play a crucial role in the responses of plants to biotic and abiotic stresses [78]. In this study, 9 TF families associated with stress were analyzed. The R2R3-MYB TF of arabidopsis *AtMYB4* plays a vital role in regulating phenylpropanoid metabolism and also participates in abiotic stress responses [79]. In this study, compared with RLC, 46 MYB family genes were upregulated (19 downregulated) in RLH and RLM. AP2/ERF TF family is one of the major cold-stress-related TF families in plants. Together with other TF families including WRKY, bHLH, bZIP, and MYB, it enhances cold stress tolerance in plants [80]. Compared with HLM, 46 AP2/ERF family TFs were upregulated and 4 were downregulated in this study. WRKY TFs are reported to be involved in response to various biotic or abiotic treatments [81]. In *A. thaliana*, it is reported that WRKY71 is involved

in regulating the ROS, SA, and jasmonic acid signaling pathways, which may promote the adaptation of plants to various abiotic stresses [82]. In this study, compared with RLC, 31 WRKY family genes were upregulated (1 was downregulated) in RLH and RLM. Among them, upregulation of *Rhe029954* (homologous to WRKY71) during HTS indicated its potential regulatory mechanism in HSR (Fig. 6). Moreover, it was observed that some members of the WRKY and AP2 families were upregulated under moderate heat stress (RLM), but downregulated under high heat stress (RLH). This phenomenon may be related to the response mechanism of plants under different heat stress levels. This discrepancy might suggest that the transcription factors are responsive to heat stress in a dose-dependent manner, with some members of these families being more strongly upregulated at moderate stress levels and potentially reaching a saturation point or undergoing downregulation when the heat stress becomes more severe. This phenomenon could be indicative of a feedback mechanism or a cellular adjustment to prevent overexpression of stress-related genes under prolonged high stress conditions [83–84]. NAC TFs is a large family involved in various processes of plants, such as growth, development, and tolerance to stress [85]. In this study, 2 NAC family genes were upregulated. HSFs play an important role in the signal transduction cascade, activating the genes of heat-induced response and acting as key TFs in the regulatory network of heat-induced response [16]. A total of three HSF genes were identified in *Rhl* including *Rhe007074*, *Rhe012339*, and *Rhe020232*, which were significantly upregulated under HS. Therefore, these TF families might be the key regulators of HS response pathways in *Rhl*.

#### Heat stress increases metabolism and expression of genes of flavonoid biosynthesis and ABC transport pathway in *Rhl*

To obtain more comprehensive understanding of the metabolic processes and gene expression regulation mechanisms of *Rhl* under HTS, combined transcriptome and metabolome analysis was conducted. As a class of important plant secondary metabolites, flavonoid compounds play a crucial role in physiological and biochemical reactions, growth and development, stress, and stress responses in plants [86]. In this study, KEGG pathway enrichment analysis revealed that flavonoid biosynthesis was significantly enriched after HTS (Fig. 5A), and 2 DEMs and 19 DEGs related to flavonoid biosynthesis were obtained (Figs. 7 and 8). Among the 2 DEMs, kaempferol positively correlated with *Rhe002395* and *Rhe022609* (correlation coefficients: 0.6761 and 0.8052, respectively;  $P$ -value < 0.001), but quercetin negatively correlated with them. Flavanone 3-hydroxylase (F3H) is one of the main factors in flavonoid biosynthesis.

Heterologous expression of DoF3H in *Escherichia coli* led to higher cold and salt stress tolerance [87]. Two F3H genes were reported in 19 DEGs, and HTS increased the expression levels of these two F3H genes (Fig. 8). These results indicated that these genes involved in the flavonoid synthesis pathway may enhance the high temperatures response of *Rhl*, and the increased synthesis of certain metabolites might improve adaptation to heat stress.

The ABC transporters that have been extensively studied in plants are the ABCB, ABCC, and ABCG subgroups. In *A. thaliana*, the main function of the ABCB subfamily is to transport secondary metabolites and hormones and control stomata opening and closing. Moreover, ABCC subfamily is reported to be involved in glucose and chlorophyll metabolism in *A. thaliana* [88, 89]. It was reported that *CsABCC1*, a major regulatory gene of the ABC transport pathway, may cause the accumulation of amino acids and carbohydrate metabolites and participate in the response to HTS [90]. In this study, the correlation analysis of DEGs and DEMs under HS revealed that *Rhe018087* and *Rhe021651* were highly positively correlated with L-isoleucine, L-leucine, and L-proline (Fig. 9). It can be concluded that the process of HTS causes changes in ABC transport metabolic pathway, and high temperature induces the increase in expression levels of *Rhe018087* and *Rhe021651*, and the accumulation of amino acids including L-proline. *Rhe018087* and *Rhe021651* may be involved in the response to HTS. It was observed that many high-temperature-responsive elements in *Cajanus cajan*, such as *CcABCG7*, *CcABCG14*, and *CcABCG32* were significantly upregulated under HTS at 42 °C [88]. ABCG transporters could positively affect plant's response to adversity by transporting specific substances, however no ABCG-related DEG was identified in the ABC transport pathway of *Rhl*, which may be attributed to the differences in growth environment and species.

#### Conclusions

In this study, 78 DEMs were screened by metabolome analysis after treating *Rhl* seedlings to various temperatures. The alterations in the expression of metabolites in RLH vs. RLM and RLH vs. RLC were greater than those in RLM vs. RLC. In total, 6.798 Gb clean data were acquired via RNA-seq, and 8450 DEGs were identified by comparison. KEGG pathway enrichment analysis revealed that DEGs in RLH vs. RLC were mainly enriched in photosynthesis, secondary metabolic biosynthesis, flavonoid biosynthesis, and other pathways. Mining of DEGs revealed that the expression of some genes related to heat stress function increased highly significantly, e.g., Gst-related gene *Rhe008987* (Log2 2.3097), HSP70-related gene *Rhe013774* (Log2 2.6519),

CHS encoding gene *Rhe001827* (Log2 9.7935), POD encoding gene by *Rhe016769* (Log2 8.1921), and ADH1-encoding gene *Rhe008676* (3.8776) associated with glycolysis/ gluconeogenesis. This needs to be further studied. Correlation analysis of metabolome and transcriptome revealed that 12 metabolic pathways were enriched in three comparison groups. In the flavonoid biosynthesis pathway, high temperature inhibited the expression of *Rhe022609* (FLS); decreased the expression of kaempferol; induced the expression of *Rhe006335*(FLS), *Rhe016929*(FL3H), and other genes; and accumulated quercetin, which improved the stress tolerance of *Rhl* under HTS. In the ABC transport pathway, high temperature induced the expression of *Rhe018087* (ABCB10) and *Rhe021651*(ABCB19), resulting in the accumulation of L-proline and other metabolites. This suggested that *Rhe018087* and *Rhe021651* are involved in the response to HTS. This study laid a solid foundation for the detailed understanding of the physiological and molecular responses of *Rhl* to HTS.

### Supplementary Information

The online version contains supplementary material available at <https://doi.org/10.1186/s12870-025-06305-3>.

Supplementary Material 1

Supplementary Material 2

Supplementary Material 3

Supplementary Material 4

Supplementary Material 5

Supplementary Material 6

Supplementary Material 7

### Acknowledgements

The authors would like to thank all the reviewers who participated in the review, as well as MJEditor ([www.mjeditor.com](http://www.mjeditor.com)) for providing English editing services during the preparation of this manuscript.

### Author contributions

Y.H.L. Methodology, Investigation, Funding acquisition, Writing—original draft, Validation. X.F.L. Conceptualization, Investigation, Methodology. M.X.L. Data curation, Investigation, Writing—original draft. J.W.H. Data curation, Methodology, Supervision. Z.M.H. Data curation, Investigation, Methodology. K.Z. Data curation, Methodology. Y.F.Y. Conceptualization, Project administration, Supervision. N.Y. Investigation, Software, Visualization Conduct. X.L.Y. Conceptualization, Project administration, Supervision. X.J.Z. Data curation, Methodology, Supervision, Writing—review & editing.

### Funding

This work was funded by the National Natural Science Foundation of China, grant number 31870697, Key Scientific Research Projects of Higher Education Institutions in Henan Province (24A180017), Innovative Training Program for College Students of Henan Province (202410482046), Natural Science Foundation of Henan Province (222300420243), and Henan Province science and technology research project (242102110326).

### Data availability

The original transcriptome sequencing data have been submitted to the NCBI BioProject database with login number: PRJNA1141191.

### Declarations

#### Ethics approval and consent to participate

Not applicable.

#### Consent for publication

Not applicable.

#### Competing interests

The authors declare no competing interests.

#### Clinical trial number

Not applicable.

Received: 3 November 2024 / Accepted: 25 February 2025

Published online: 04 March 2025

### References

- Huylenbroeck J. Ornamental crops. Springer International, Publishing AG. Cham 2018; 237–271. <https://doi.org/10.1007/978-3-319-90698-0>
- Liu N, Zhang L, Zhou Y, Tu M, Wu Z, Gui D, Ma Y, Wang J, Zhang C. The rhododendron plant genome database (rpgd): a comprehensive online omics database for rhododendron. BMC Genom. 2021;22:376. <https://doi.org/10.1186/s12864-021-07704-0>.
- Lin W, Liu L, Liang JC, Tang XX, Shi J, Zhang L, Wu PR, Lan SR, Wang SS, Zhou Y, et al. Changes of endophytic microbial community in Rhododendron Simsii roots under heat stress and its correlation with leaf physiological indicators. Front Microbiol. 2022;13:1006686. <https://doi.org/10.3389/fmicb.2022.1006686>.
- Zhou XJ, Wang HL, Li FL, Zhang K, Wang YN, Ya HY. Development of polymorphic SSR markers in *Rhododendron Henanense* subsp. *Lingbaoense* based on RAD-seq. J Agric Biotech. 2019;27:55–62. <https://doi.org/10.3969/j.issn.1674-968.2019.01.006>.
- Ye YZ, Wang WS, Li HS. Henan Xiaoqinling National nature reserve scientific investigation collection. Beijing: Science; 2004.
- Yue FN, Han TY, Zhang YF. Investigation of habitat conditions, protection and utilization of germplasm resources of Rhododendron henanense subsp. Lingbaoense, Spec. Economic Plants Animals. 2019;(22):22–25.
- Gao XM, Shi SL. Evaluations on the ornamental characteristics of the rare and threatened plants in Henan. J Bot Res. 1995;13:87–94.
- White SM, Shelton CL, Gelb AW, Lawson C, McGain F, Muret J, Sherman JD, McGain F, Muret J, Lawson C, et al. Principles of environmentally-sustainable anaesthesia: a global consensus statement from the world federation of societies of anaesthesiologists. Anaesthesia. 2022;77:201–12. <https://doi.org/10.1111/anae.15598>.
- Rillig MC, Ryo M, Lehmann A, Aguilar-Trigueros CA, Buchert S, Wulf A, Iwasaki A, Roy J, Yang G. The role of multiple global change factors in driving soil functions and microbial biodiversity science. 2019;366(6467):886–90.
- Lin W, Ye Q, Liang J, et al. Response mechanism of interaction between Rhododendron Hainanense and microorganisms to heat stress[J]. Ind Crops Prod. 2023;199:116764.
- Kumar RR, Rai GK, Kota S, Watts A, Sakhare A, Kumar S, Goswami S, Kapoor N, Babu P, Mishra GP, et al. Fascinating dynamics of silicon in alleviation of heat stress induced oxidative damage in plants. Plant Growth Regul. 2023;100:321–35. <https://doi.org/10.1007/s10725-022-00879-w>.
- Azameti MK, Ranjan A, Singh PK, Gaikwad K, Singh AK, Dalal M, Arora A, Rai V, Padaria JC. Transcriptome profiling reveals the genes and pathways involved in thermotolerance in wheat (*Triticum aestivum* L.) genotype Raj 3765. Sci Rep. 2022;12:14831. <https://doi.org/10.1038/s41598-022-18625-7>.
- Scharf KD, Berberich T, Ebersberger I, Nover L. The plant heat stress transcription factor (Hsf) family: structure, function and evolution. Biochim Biophys Acta Gene Regul Mech. 2012;1819:104–19. <https://doi.org/10.1016/j.bbagr.2011.10.002>.
- Anwar M, Saleem MA, Dan M, Malik W, Ul-Allah S, Ahmad MQ, Qayyum A, Amjid MW, Zia ZU, Afzal H, Hammad A, Asif M, Ur Rahman MA, Hua ZL. Morphological, physiological and molecular assessment of cotton for drought tolerance under field conditions. Saudi J Biol Sci. 2022;29:444–52. <https://doi.org/10.1016/j.sjbs.2021.09.009>



15. Zha Q, Yin XJ, Xi XJ, Jiang AL. Heterologous VvDREB2c expression improves heat tolerance in Arabidopsis by inducing photoprotective responses. *Int J Mol Sci*. 2023;24:5989. <https://doi.org/10.3390/ijms24065989>.
16. Ohama N, Sato H, Shinozaki K, Yamaguchi-Shinozaki K. Transcriptional regulatory network of plant heat stress response. *Trends Plant Sci*. 2017;22:53–65. <https://doi.org/10.1016/j.tplants.2016.08.015>.
17. Kotak S, Larkindale J, Lee U, von Koskull-Döring P, Vierling E, Scharf KD. Complexity of the heat stress response in plants. *Curr Opin Plant Biol*. 2007;10:310–6. <https://doi.org/10.1016/j.pbi.2007.04.011>.
18. Wahid AS, Gelani M, Ashraf MR, Foolad. Heat tolerance in plants: an overview. *Environ Exp Bot*. 2007;61:199–223. <https://doi.org/10.1016/j.envexpbot.2007.05.011>.
19. Mittler R, Finka A, Goloubinoff P. How do plants feel the heat? *Trends Biochem Sci*. 2012;37:118–25.
20. Lobell DB, Schlenker W, Costa-Roberts J. Climate trends and global crop production since 1980. *Science*. 2011;333:616–20. <https://doi.org/10.1126/science.120453>.
21. Jiang JC. Effects of High Temperature Stress on the Growth and Physiology of Three Rhododendron Species. Master's Thesis. Central South University of Forestry and Technology, Changsha, China, 2023.
22. Chen C, Zheng Y, Zhong Y, Wu Y, Li Z, Xu LA, Xu M. Transcriptome analysis and identification of genes related to terpenoid biosynthesis in *cinnamomum camphora*. *BMC Genomics*. 2018;19:1–15. <https://doi.org/10.1186/s12864-018-4941-1>.
23. Yang H, Gu X, Ding M, Lu W, L. D. Heat stress during grain filling affects activities of enzymes involved in grain protein and starch synthesis in waxy maize. *Sci Rep*. 2018;8:15665. <https://doi.org/10.1038/s41598-018-33644-z>.
24. Jiao Z, Xu W, Nong Q, Zhang M, Jian S, Lu H, Chen J, Zhang M, Xia K. An integrative transcriptomic and metabolomics analysis of red Pitaya (*Hylocereus polyrhizus*) seedlings in response to heat stress. *Genes*. 2021;12:1714. <https://doi.org/10.3390/genes12111714>.
25. Wienkoop S, Morgenthal K, Wolschi F, Scholz M, Selbig J, Wolfram, Weckwerth. Integration of metabolomic and proteomic phenotypes: analysis of data covariance dissects starch and RFO metabolism from low and high temperature compensation response in *arabidopsis thaliana*. *Mol Cell Proteom*. 2008;7:1725–36.
26. Pan XD, Wang JW, Hu Y, Chi Y, Jin SH. Physiological and biochemical responses of leaves of four Rhododendron cultivars under heat stress, *mol. Plant Breed*. 2022;20:6877–84. <https://doi.org/10.13271/j.mpb.020.006877>.
27. Park CH, Yeo HJ, Kim NS, Park YE, Park SY, Kim JK, Park SU. Metabolomic profiling of the white, Violet, and red flowers of Rhododendron schlippenbachii Maxim. *Molecules*. 2018;23:827. <https://doi.org/10.3390/molecules23040827>.
28. Wu HR. Regeneration system of three variety Rhododendron in vitro. Master's Thesis. Guizhou University, Guizhou, China, 2023.
29. Liu XJ, Su HG, Peng XR, Bi HC, Qiu MH. An updated review of the genus Rhododendron since 2010: traditional uses, phytochemistry, and Pharmacology. *Phytochemistry*. 2024;217:113899. <https://doi.org/10.1016/j.phytochem.2023.113899>.
30. Guo XM, Yan XY, Li YH. Genome-wide identification and expression analysis of the WRKY gene family in Rhododendron henanense subsp. lingbaoense. *PeerJ*. 2023; (12): e17435. <https://doi.org/10.7717/peerj.17435>.
31. Liu Y, Fan H, Dong J, Chen J, Xu H, Zhou X. Phosphoproteomics of cold Stress-Responsive mechanisms in *Rhododendron Chrysanthum*. *Mol Biol Rep*. 2022;49:303–12. <https://doi.org/10.1007/s11033-021-06874-0>.
32. Xu SD, Geng XM, Mao LF, Yi Y, Gong JY, Xu XR. Transcriptome analysis and identification of the genes associated with the heat stress response in four rhododendron species. *Sci Hortic*. 2022;303:111176. <https://doi.org/10.1016/j.scienta.2022.111176>.
33. Zhou XJ, Li JT, Wang HL, Han JW, Zhang K, Dong SW, Zhang YZ, Ya HY, Cheng YW, Sun SS. The chromosome-scale genome assembly, annotation and evolution of Rhododendron henanense subsp. lingbaoense. *Mol. Ecol. Resour*. 2022; (22):988–1001. <https://doi.org/10.1111/1755-0998.13529>.
34. Li Y, Ma H, Chen S, Chen Y, Zhou X, Yu X, Zhang Y, Han J, Wang H. Genome-wide Elucidation and expression features of Q-type C2H2 zinc finger protein gene family in Rhododendron Henanense subsp. Lingbaoense. *Genet Resour Crop Evol*. 2024;1–20. <https://doi.org/10.1007/s10722-024-02030-2>.
35. Rasmussen JA, Villumsen KR, Ernst M, Hansen M, Forberg T, Gopalakrishnan S, Gilbert MTP, Bojesen AM, Kristiansen K, Limborg MTA. multi-omics approach unravels metagenomic and metabolic alterations of a probiotic and synbiotic additive in rainbow trout (*Oncorhynchus mykiss*). *Microbiome*. 2022;10:21. <https://doi.org/10.1186/s40168-021-01221-8>.
36. Navarro-Reig M, Jaumot J, García-Reiriz A, Tauler R. Evaluation of changes induced in rice metabolome by Cd and Cu exposure using LC-MS with XCMS and MCR-ALS data analysis strategies. *Anal Bioanal Chem*. 2015;407:8835–47. <https://doi.org/10.1007/s00216-015-9042-2>.
37. Horai H, Arita M, Kanaya S, Nihei Y, Ikeda T, Suwa K, Ojima Y, Tanaka K, Tanaka S, Aoshima K, et al. MassBank: a public repository for sharing mass spectral data for life sciences. *J Mass Spectrom*. 2010;45:703–14. <https://doi.org/10.1002/jms.1777>.
38. Wishart DS, Tzur D, Knox C, Eisner R, Guo AC, Young N, Cheng D, Jewell K, Arndt D, Sawhney S, et al. Querengesser, HMDB: the human metabolome database. *Nucleic Acids Res*. 2007;35:521–6. <https://doi.org/10.1093/nar/gkl923>.
39. Ogata H, Goto S, Sato K, Fujibuchi W, Bono H, Kanehisa M. KEGG: Kyoto encyclopedia of genes and genomes. *Nucleic Acids Res*. 1999;27:29–34. <https://doi.org/10.1093/nar/27.1.29>.
40. Thévenot EA, Roux A, Xu Y, Egan E, Junot C. Analysis of the human adult urinary metabolome variations with age, body mass index, and gender by implementing a comprehensive workflow for univariate and OPLS statistical analyses. *J Proteome Res*. 2015;14:3322–35. <https://doi.org/10.1021/acs.jproteome.5b00354>.
41. Kieffer DA, Piccolo BD, Vaziri ND, Liu S, Lau WL, Khazaeli M, Nazertehrani S, Moore ME, Marco ML, Martin RJ, et al. Resistant starch alters gut Microbiome and metabolomic profiles concurrent with amelioration of chronic kidney disease in rats. *Am J Physiol Ren Physiol*. 2016;310:857–71. <https://doi.org/10.1152/ajprenal.00513.2015>.
42. Xia J, Wishart DS. Web-based inference of biological patterns, functions and pathways from metabolomic data using metaboanalyst. *Nat Protoc*. 2011;6:743–60. <https://doi.org/10.1038/nprot.2011.319>.
43. Martin DM, Fäldt J, Bohlmann J. Functional characterization of nine Norway Spruce TPS genes and evolution of gymnosperm terpene synthases of the TPS-d subfamily. *Plant Physiol*. 2004;135:1908–27. <https://doi.org/10.1104/pp.104.042028>.
44. Li CH, Zhang JY, Zhang XY, Li SH, Gao JM. An overview of grayanane diterpenoids and their biological activities from the Ericaceae family in the last seven years. *Eur J Med Chem*. 2019;166:400–16. <https://doi.org/10.1016/j.ejmech.2019.01.079>.
45. Popescu R, Kopp B. The genus rhododendron: an ethnopharmacological and toxicological review. *J Ethnopharmacol*. 2013;147:42–62. <https://doi.org/10.1016/j.jep.2013.02.022>.
46. Zha HG, Milne RI, Zhou HX, Chen XY, Sun H. Identification and cloning of class II and III chitinases from alkaline floral nectar of *Rhododendron irroratum*. *Ericaceae Planta*. 2016;244:805–18. <https://doi.org/10.1007/s00425-016-2546-y>.
47. Zhu YX, Zhang ZX, Yan HM, Lu D, Zhang HP, Li L, Liu YB, Li Y. Antinociceptive diterpenoids from the leaves and twigs of rhododendron decorum. *J Nat Prod*. 2018;81:1183–92. <https://doi.org/10.1021/acs.jnatprod.7b00941>.
48. Shi Y, Zhou M, Zhang Y, Fu Y, Li J, Yang X. Poisonous delicacy: market-oriented surveys of the consumption of Rhododendron flowers in Yunnan. *China J Ethnopharmacol*. 2021;265:113320. <https://doi.org/10.1016/j.jep.2020.113320>.
49. Luo SY, Xu QH, Peng G, Chen ZW. The protective effect of total flavones from *Rhododendron Simsii* planch. On myocardial ischemia/reperfusion injury and its underlying mechanism, *evid. Based Complement Alternat Med*. 2018;6139372. <https://doi.org/10.1155/2018/6139372>.
50. Maestri E, Klueva N, Perrotta C, Gulli M, Nguyen HT, Marmiroli N. Molecular genetics of heat tolerance and heat shock proteins in cereals. *Plant Mol Biol*. 2022;48:667–81. <https://doi.org/10.1023/A:1014826730024>.
51. Scharf KD, Berberich T, Ebersberger I, Nover L. The plant heat stress transcription factor (Hsf) family: structure, function and evolution. *Biochim Biophys Acta Gene Regul Mech*. 2012;1819:104–19. <https://doi.org/10.1016/j.bbagr.2011.10.002>.
52. Hayat S, Hayat Q, Alyemeni MN, Wani AS, Pichtel J, Ahmad A. Role of proline under changing environments. *Plant Signal Behav*. 2012;7:1456–66. <https://doi.org/10.4161/psb.21949>.
53. Zhao Q, Chen W, Bian J, Xie H, Li Y, Xu C, Ma J, Guo S, Chen J, Cai X, et al. Proteomics and phosphoproteomics of heat Stress-Responsive mechanisms in spinach, *front. Plant Sci*. 2018;9:800. <https://doi.org/10.3389/fpls.2018.00800>.
54. Apak R, Özyürek M, Güçlü K, Çapanoğlu E. Antioxidant activity/capacity measurement. 2. Hydrogen atom transfer (hat)-based, mixed-mode (electron transfer (ET)/HAT), and lipid peroxidation assays. *J Agric Food Chem*. 2016;64:1028–45. <https://doi.org/10.1021/acs.jafc.5b04743>.

55. Zhao Y, Yu W, Hu X, Shi Y, Liu Y, Zhong Y, Wang P, Deng S, Niu J, Yu X. Physiological and transcriptomic analysis revealed the involvement of crucial factors in heat stress response of *Rhododendron hainanense*. *Gene*. 2018; (660):109–119. <https://doi.org/10.1016/j.gene.2018.03.082>
56. Geng X, Mao L, Yi Y, Gong J, Xu X. Transcriptome analysis and identification of the genes associated with the heat stress response in four rhododendron species. *Sci Hortic*. 2022;303:111176. <https://doi.org/10.1016/j.scienta.2022.111176>.
57. Li SP, Deng BL, Tian S, Guo MX, Liu HX, Zhao XS. Metabolic and transcriptomic analyses reveal different metabolite biosynthesis profiles between leaf buds and mature leaves in *Ziziphus jujuba* mill. *Plants*. 2020;9:871.
58. Zhang J, Li XM, Lin HX, Chong K. Crop improvement through temperature resilience. *Annu Rev Plant Biol*. 2019;70:753–80. <https://doi.org/10.1146/annurev-arplant-050718-100016>.
59. Zandalinas SI, Fichman Y, Deviredy AR, Sengupta S, Azad RK, Mittler R. Systemic signaling during abiotic stress combination in plants. *P Natl Acad Sci USA*. 2020;117:13810–20. <https://doi.org/10.1073/pnas.2005077117>.
60. Singh B, Kukreja S, Goutam U. Impact of heat stress on potato (*Solanum tuberosum* L.): present scenario and future opportunities. *J Hortic Sci Biotech*. 2020;95:407–24. <https://doi.org/10.1080/14620316.2019.1700173>.
61. Baxter A, Mittler R, Suzuki N. ROS as key players in plant stress signaling. *J Exp Bot*. 2014;65:1229–40. <https://doi.org/10.1093/jxb/ert375>.
62. Belhadj Slimen I, Najar T, Ghrum A, Dabbabi H, Ben Mrad M, Abdrabbah M. Reactive oxygen species, heat stress and oxidative-induced mitochondrial damage. *Int J Hyperth*. 2014;30:513–23. <https://doi.org/10.3109/02656736.2014.971446>.
63. Nadarajah KK. ROS homeostasis in abiotic stress tolerance in plants. *Int J Mol Sci*. 2020;21:5208. <https://doi.org/10.3390/ijms21155208>.
64. Wang J, Lv J, Liu Z, Liu Y, Song J, Ma Y, Ou L, Zhang X, Liang C, Wang F, et al. Integration of transcriptomics and metabolomics for pepper (*Capsicum annuum* L.) in response to heat stress. *Int J Mol Sci*. 2019;20:5042. <https://doi.org/10.3390/ijms20205042>.
65. Tiwari M, Kumar R, Min D, Jagadish SVK. Genetic and molecular mechanisms underlying root architecture and function under heat stress—a hidden story. *Plant Cell Environ*. 2022;45:771–88. <https://doi.org/10.1111/pce.14266>.
66. Cai JH, Chen YH, Lai JL, Zheng W, Hu JT, Liu SY, Luo SM, Liu XP, Guo RS. Evaluation on heat resistance of 18 rhododendrons. *Mod Hortic*. 2022;45:6–9.
67. Calzadilla PI, Signorelli S, Escaray FJ, Menéndez AB, Monza J, Ruiz OA, Maiale SJ. Photosynthetic responses mediate the adaptation of two *Lotus japonicus* ecotypes to low temperature. *Plant Sci*. 2016;250:59–68. <https://doi.org/10.1016/j.plantsci.2016.06.003>.
68. Liu H, Huang RYC, Chen J, Gross ML, Pakrasi HB. Psb27, a transiently associated protein, binds to the chlorophyll binding protein CP43 in photosystem II assembly intermediates. *Proc Natl Acad Sci*. 2011;108:18536–41. <https://doi.org/10.1073/pnas.111159710>.
69. Sakata S, Mizusawa N, Kubota-Kawai H, Sakurai I, Wada H. Psb28 is involved in recovery of photosystem II at high temperature in *Synechocystis* Sp. PCC 6803. *biochim. Biophys Acta Bioenerg*. 2013;1827:50–9. <https://doi.org/10.1016/j.bbabi.2012.10.004>.
70. Song YP, Chen QQ, Ci D, Shao XN, Zhang DQ. Effects of high temperature on photosynthesis and related gene expression in Poplar. *BMC Plant Biol*. 2014;14:111. <http://www.biomedcentral.com/1471-2229/14/111>.
71. George IS, Pascovici D, Mirzaei M, Haynes PA. Quantitative proteomic analysis of *Cabernet sauvignon* grape cells exposed to thermal stresses reveals alterations in sugar and phenylpropanoid metabolism. *Proteomics*. 2015;15:3048–60. <https://doi.org/10.1002/pmic.201400541>.
72. Miller GAD, Mittler RON. Could heat shock transcription factors function as hydrogen peroxide sensors in plants. *Ann. Bot*. 2006;279–288. <https://doi.org/10.1093/aob/mcl107>
73. Banilas G, Korkas E, Englezos V, Nisioutou AA, Hatzopoulos P. Genome-wide analysis of the heat shock protein 90 gene family in grapevine (*Vitis vinifera* L.). *Aust J Grape Wine Res*. 2012;18:29–38. <https://doi.org/10.1111/j.1755-0238.2011.00166.x>.
74. Maestri E, Klueva N, Perrotta C, Gulli M, Nguyen HT, Marmiroli N. Molecular genetics of heat tolerance and heat shock proteins in cereals. *Plant Mol Biol*. 2002;48:667–81. <https://doi.org/10.1023/A:1014826730024>.
75. Xue J, Zeng P, Cui J, Zhang Y, Yang J, Zhu L, Hu H, Xu J. Physiological and gene expression changes of *Cryptomeria Fortunei* Hooibrenk families under heat stress. *front. Plant Sci*. 2023;14:1083847. <https://doi.org/10.3389/fpls.2023.1083847>.
76. Ireland HE, Harding SJ, Bonwick GA, Jones M, Smith CJ, Williams JHH. Evaluation of heat shock protein 70 as a biomarker of environmental stress in *Fucus serratus* and *Lemna minor*. *Biomarkers*. 2004;9:139–55. <https://doi.org/10.1080/13547500410001732610>.
77. Cai Z, He F, Feng X, Liang T, Wang H, Ding S, Tian X. Transcriptomic analysis reveals important roles of lignin and flavonoid biosynthetic pathways in rice thermotolerance during reproductive stage. *front. Genet*. 2020;11:562937. <https://doi.org/10.3389/fgene.2020.562937>.
78. Zhou Q, Luo D, Chai X, Wu Y, Wang Y, Nan Z, Yang Q, Liu W, Liu Z. Multiple regulatory networks are activated during cold stress in *Medicago sativa* L. *Int J Mol Sci*. 2018;19:3169. <https://doi.org/10.3390/ijms19103169>.
79. Li Y, Shi Y, Li M, Fu D, Wu S, Li J, Gong Z, Liu H, Yang S. The CRY2-COP1-HY5-BBX7/8 module regulates blue light-dependent cold acclimation in Arabidopsis. *Plant Cell*. 2021;33:3555–73. <https://doi.org/10.1093/plcell/koab215>.
80. Ritonga FN, Ngatia JN, Wang Y, Khoso MA, Farooq U, Chen S. AP2/ERF, an important cold stress-related transcription factor family in plants: A review. *physiol. Mol Biol Plant*. 2021;27:1953–68. <https://doi.org/10.1007/s12298-021-01061-8>.
81. Bakshi M, Oelmüller R. WRKY transcription factors: Jack of many trades in plants. *Plant Signal Behav*. 2014;9:e27700. <https://doi.org/10.4161/psb.27700>.
82. Guo D, Qin G. EXB1/WRKY71 transcription factor regulates both shoot branching and responses to abiotic stresses. *Plant Signal Behav*. 2016;11:e1150404. <https://doi.org/10.1080/15592324.2016.1150404>.
83. Bakery A, Vraggalas S, Shalha B, Chauhan H, Benhamed M, Fragkostefanakis S. Heat stress transcription factors as the central molecular rheostat to optimize plant survival and recovery from heat stress. *New Phytol*. 2024;244(1):51–64. <https://doi.org/10.1111/nph.20017>.
84. Tao H, Xu SC, Shen HL, Yang JW, Xu YY, Huang GP, Feng CQ, Wan WF, Woldegiorgis ST, Liu W, He HQ. Genome-wide characterization and functional analysis of heat shock transcription factors in wild and cultivated rice (*Oryza sativa* L.). *Plant Stress*. 2024; (12):100505. <https://doi.org/10.1016/j.stress.2024.100505>
85. Fang Y, You J, Xie K, Xie W, Xiong L. Systematic sequence analysis and identification of tissue-specific or stress-responsive genes of NAC transcription factor family in rice. *Mol Gen Genomics*. 2008;280:547–63. <https://doi.org/10.1007/s00438-008-0386-6>.
86. Harborne JB, Williams CA. Advances in flavonoid research since 1992. *Phytochemistry*. 2000;55:481–504. [https://doi.org/10.1016/S0031-9422\(00\)00235-1](https://doi.org/10.1016/S0031-9422(00)00235-1).
87. Dong C, Si W, da Silva JAT, He C, Yu Z, Zhang M, Huang L, Zhao C, Zeng D, Li C, Qiu S, et al. Functional analysis of Flavanone 3-hydroxylase (F3H) from *Dendrobium officinale*, which confers abiotic stress tolerance. *Hortic Plant J*. 2023;9:356–64. <https://doi.org/10.1016/j.hpj.2022.03.006>.
88. Schulz B, Kolukisaoglu HÜ. Genomics of plant ABC transporters: the alphabet of photosynthetic life forms or just holes in membranes? *FEBS Lett*. 2006;580:1010–6. <https://doi.org/10.1016/j.febslet.2006.01.002>.
89. Niu L, Li H, Song Z, Dong B, Cao H, Liu T, Du T, Yang W, Amin R, Wang L, et al. The functional analysis of ABCG transporters in the adaptation of pigeon pea (*Cajanus cajan*) to abiotic stresses. *PeerJ*. 2021;9:e10688. <https://doi.org/10.7717/peerj.10688>.
90. Zheng S, Liu C, Zhou Z, Xu L, Lai Z. Physiological and transcriptome analyses reveal the protective effect of exogenous Trehalose in response to heat stress in tea plant (*Camellia sinensis*), plants. 2024;13:1339. <https://doi.org/10.3390/plants1310133>

## Publisher's note

Springer Nature remains neutral with regard to jurisdictional claims in published maps and institutional affiliations.